PERFORMANCE ANALYSIS OF SOLAR PHOTOVOLTAIC THERMAL HYBRID SYSTEM

A

Dissertation

Submitted in partial fulfillment of the

Requirement of the award of degree

of

MASTER OF TECHNOLOGY

in

ALTERNATE HYDRO ENERGY SYSTEMS

By

HIMANSHU MISHRA

DEPARTMENT OF HYDRO AND RENEWABLE ENERGY

INDIAN INSTITUTE OF TECHNOLOGY

ROORKEE-247667 (INDIA)

JUNE 2019

CANDIDATE'S DECLARATION

I hereby declare that the work which is being presented in this dissertation entitled **"PERFORMANCE ANALYSIS OF HYBRID SOLAR PHOTOVOLTAIC THERMAL SYSTEM"** in partial fulfillment of the requirements for the award of the degree of **Master of Technology** with specialization in **Alternate Hydro Energy Systems**, submitted in **Department of Hydro and Renewable Energy (HRED), Indian Institute of Technology Roorkee, Uttarakhand, India**, is an authentic record of my own work carried out under the supervision of **Dr. R.P. Saini**, Professor, Department of Hydro and Renewable Energy, Indian Institute of Technology Roorkee, India.

I have not submitted the matter embodied in this dissertation report for the award of any other degree or diploma.

Date: **(HIMANSHU MISHRA)**

CERTIFICATE

This is to certify that the above statement made by the candidate is correct to the best of my knowledge.

(Dr. R.P. Saini)
Professor
Department of Hydro and Renewable Energy
Indian Institute of Technology
Roorkee -247667

ABSTRACT

Solar energy is a safe alternative that can replace current fossil fuels, like coal and gas for generation of electricity that produce air, water, and land pollution. World Wide Fund for Nature (WWF), noted that electricity generation from fossil fuels causes pollution of air leading to acid rain, damaged forest areas, and affected agricultural production. Similarly, nuclear power also pollutes water and land, but the use of solar energy can replace these conventional fossil fuels. Solar energy can be converted directly into electrical energy with the help of P-V generator, and this electrical energy is a high grade energy which can be converted into any other form of energy as per the requirement. To utilize the solar energy, there is a need of more efficient system, because solar energy is a dilute form of energy.

Hybrid Solar Photo voltaic thermal system (HPVT) can be used to achieve better efficiency with more energy output. HPVT system produces electricity and also uses the thermal energy of a heated solar panel, which is going to be waste in the form of conduction and convection losses. Utilization of thermal energy increases the overall efficiency of system by increasing the net output of system as well as increase the efficiency of PV generator by reducing its temperature.

Under the present dissertation work different types of HPVT systems are analyzed for various modified designs. To modify the design for better performance, several parameters are selected to increase the heat transfer rate in HPVT system. This report also presents the CFD analysis of these modified systems, and comparison among these systems. During the performance analysis of HPVT system, it is found that the maximum reduction in panel temperature is 9.2 ℃, in case of cubical shaped protrusions, which further increase the electrical (PV) efficiency by an amount of 4.8 %. It is also observed that HPVT systems with discontinuous roughness (cubical and spherical shaped protrusions, having a system efficiency of 25.70% and 24.77% respectively) are more efficient than the systems having continuous ribs (longitudinal, transverse and inclined ribs which have an efficiency of 20.94 %, 21.58 % and 23.7% respectively) at a maximum mass flow rate of 0.069 kg/s.

ACKNOWLEDGEMENTS

I would like to express my sincere gratitude to my guide **Dr. R.P. Saini**, Professor, Department of Hydro and Renewable Energy, Indian Institute of Technology Roorkee, for his valuable guidance, support, encouragement, continuous inspiration, motivation and immense help during the progress of this dissertation work.

Moreover, I would remain grateful to all faculty members and staffs of Department of Hydro and Renewable Energy, Indian Institute of Technology Roorkee and also would like to extend my heartfelt thanks to all my friends who have helped me directly or indirectly for this dissertation work.

I would also like to pay my sincere gratitude to research scholar Gaurav Saini, for his support in improving the quality of the report.

At the last but not the least I would like to express my humble respect and special thanks to my parent and others who has directly or indirectly helped me during the dissertation work.

Date:

Place: Roorkee **(HIMANSHU MISHRA)**

TABLE OF CONTENT

LIST OF FIGURES

LIST OF TABLES

NOMENCLATURE

SYMBOL	DESCRIPTION	UNIT
ρ	Density of Air	kg/m^3
μ_{air}	Kinematic Viscosity of Air	Ns/m^2
D_h	Hydraulic Diameter	m
A	Area of Cross Section	m^2
V	Velocity of Air	m/s
$\dot{m}$	Mass Flow Rate	kg/s
f	Friction Factor	-
$\triangle p$	Pressure Drop	N/m^2
W_b	Blower Work Required	W
P_{max}	Maximum Power	W
V_{mp}	Maximum Power Voltage	V
I_{mp}	Maximum Power Current	A
V_{oc}	Open Circuit Voltage	V
I_{sc}	Short Circuit Current	A
α	Temperature Coefficient of Isc	mA/˚C
β	Temperature Coefficient of Voc	mV/˚C
Υ	Temperature Coefficient of P	%/˚C
E_s	Solar Energy Absorbed by Panel	W
E_p	Energy Required to Drive the Pump	W
E_e	Electrical Power Generated by Panel	W
E_f	Energy Carried Away by Fluid	W
h	Convective Heat Transfer Coefficient	W/m^2K
A	Exposed Surface Area of Panel	m^2
T_p	Panel Temperature	˚C
T_a	Ambient Temperature	˚C
I	Total Solar Radiation Falling on Panel	W/ m^2
T_i	Inlet Fluid Temperature	˚C

T_o	Outlet Fluid Temperature	˚C
$(dt)_p$	Drop in Panel Temperature	˚C
$(dt)_f$	Change in HTF Temperature	˚C
ηth	Thermal Efficiency	%
ηe	Electrical Efficiency	%
ηs	System Efficiency	%

SUBSCRIPTS

SYMBOL	**DESCRIPTION**
HPVT	Hybrid Photovoltaic Thermal.
PVT	Photovoltaic Thermal.
NOCT	Normal Operating Cell Temperature.
STC	Standard Test Condition.
CFD	Computational Fluid Dynamics.
HTF	Heat Transfer Fluid.

CHAPTER 1
INTRODUCTION

1.1 GENERAL

As the nations are developing and their energy demand is increasing continuously whereas the conventional resources to fulfill these energy requirements are vanishing continuously. The renewable energy sources are abundant and have enough potential to fulfill large part of these energy demand. Growing renewable energy sources technology has become quite accessible and their prices have fallen over the years. Renewable energy sources have the potential to provide energy with negligible emission of air pollutants and greenhouse gases. Renewable energy technologies produce saleable energy by converting natural resource. It is a promising prospect for the future as an alternative to conventional energy. Hydro power, Wind, Biomass, Solar energy are some of the sources which have proved to be promising.

The world is making an extreme effort to decrease carbon emissions and limit the change in global average temperature with a new pact decided in 2015 at the Paris Climate Summit (COP21). To move forward, we also need to realize that can possibly be done limiting GHG output as the human population only increases and puts more demands on our energy infrastructure. To further help the environment and secure the future of the planet for our next generation we need to move to renewable sources for our energy generation.

Based on REN21's 2017 report, renewables contributed 24.5% to the generation of electricity and 19.3% to humans' global energy consumption in 2015 and 2016, respectively. This energy consumption is given as 8.9 % from traditional biomass, 4.2 % as heat energy (modern biomass heat, geothermal heat and solar heat), 3.9% hydro-electricity and 2.2% is electricity from wind, solar, geothermal, and biomass.

In spite of huge potential, these are produced in a limited quantity just because of technological constraints. With improve in technology in future, it is expected that huge dependability will be on these resources. Among many renewable energy India is endowed with vast potential to provide for solar energy and is rapidly developing as a major manufacturing hub for solar power plants. Some methods to exploit solar energy are through use of P-V generator, solar water heater solar air heater, vapor absorption refrigeration system (VARS), a solar hybrid systems combined with conventional energy sources, hybrid photovoltaic thermal systems and many more.

1.2 CLASSIFICATION OF ENERGY SOURCES

Classification of solar energy can be done in following ways:

1.2.1 Non Renewable Energy Sources

The energy sources which do not replenish in a given period of time or takes millions of years to reproduce themselves, comes under this category. These energy sources are also harmful for the environment and pollute it badly. These resources are also the main cause of global warming. Some of these resources are given below.

A. Coal

a. Anthracite.
b. Bituminous.
c. Lignite.
d. Peat.

B. Oil

a. Conventional oil.
b. Heavy and extra heavy oil.
c. Shale oil.

C. Gas

a. Natural gas.
b. Shale gas.

D. Nuclear Energy

a. Fission (based on uranium).
b. Fusion (based on deuterium).

Various types of energy sources can be summarized in Fig. 1.1.

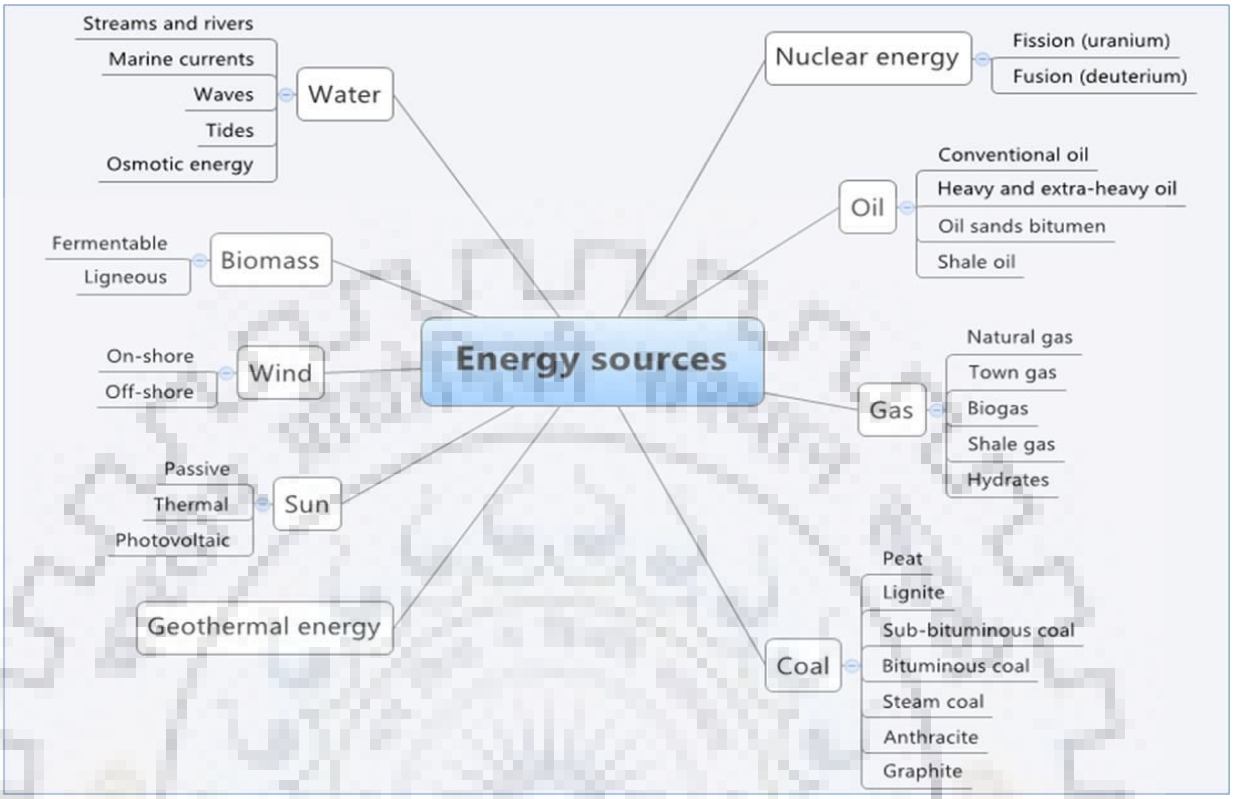

Fig. 1.1: Various Types of Energy Sources [1].

1.2.2 Renewable Energy Sources

Renewable energy is the energy collected from the natural sources, which are naturally replenished in human timespan, such as wind, sunlight, rain, tides, waves, and geothermal heat. These sources are almost pollution free and environment friendly hence zero carbon emission. As it can be observed that the temperature of environment is continuously increasing because of global warming, so all the countries decided to lower the carbon emission for controlling the global temperature up to a limit of 1.5℃ increase. So India is also contributing in this and has set its target to produce 175 GW electricity up to 2022 from renewable energy sources which are given below separately.

A. Hydro Energy

Hydropower is one of the world's largest and cheapest source of energy. It is one of the most efficient and popular way for the generation of electricity. India set its target of 5 GW electricity generation from small hydro power up to 2022. In India we consider small hydro up to 25 MW as renewable sources of energy, which may be of the following types.

a. Stored water (by making dam).

b. Flowing water (Run-off River).

c. Waves.

d. Tides.

B. Wind Energy

In wind energy India is ranked as the 4th in wind power installed capacity after China, United States and Germany. Wind power capacity of India, as of 31 March 2018, was 34,050 MW, making India as the fourth-largest wind power producer in the whole world. A recent study done by National Institute of Wind Energy (NIWE) has revealed wind energy potential of 302 GW at 100 m hub-height in India. India's target is to produce 60 GW electricity by wind energy up to 2022. Wind energy can be extracted from following ways.

a. On-shore.

b. Off-shore.

C. Biomass

Biomass is the organic material which provide the considerable amount of energy when burnt. It can be termed as getting energy by burning wood, and other organic matter which naturally exist. Carbon emissions are released while burning the biomass, but it has been classified as a renewable energy source in the EU and United Nation's legal frameworks, because plant stocks can be replainished with new growth. As an energy source, biomass can be used directly via combustion to produce heat, or it can be used indirectly after converting it to different forms of biofuel. Conversion of biomass into biofuel can be done by different methods which are classified into 3 major parts as: chemical, biochemical and thermal. Biomass can be classified mainly into two types.

a. Fermentable.

b. Ligneous (Wood etc.).

D. Geothermal Energy

Geothermal energy is thermal energy created and stored in the Earth. Thermal energy is the energy that limits the temperature of matter and geothermal gradient (difference in temperature between the core of the planet and its surface) drives a continuous conduction of thermal energy in the form of heat from the core to the surface.

E. Solar Energy

Light and heat from the sun, can be harnessed by using the ever-evolving technologies like solar heating, photovoltaics (P-V), concentrated solar power (CSP) and artificial photosynthesis. Solar technologies can be broadly categorized as passive solar technology and active solar technology, depending upon the way they collect, convert and distribute the solar energy. Passive solar techniques include orienting a building to the Sun, selecting materials with favorable thermal mass or light dispersing properties, and designing spaces that naturally circulate air. Active solar technologies encompass solar thermal energy, using solar collectors for heating, and solar power, converting sunlight into electricity either directly using photovoltaics (PV), or indirectly using concentrated solar power (CSP).

As India's location suits for the utilization of solar energy India is proving itself as a global leader in the field of solar energy, and an ambitious target of producing 100GW electricity by solar energy is set by the year 2022.

There are various alternative available for utilization of solar energy. But broadly we can use solar energy with the help of following three types of systems.

a. Photovoltaic systems

b. Thermal systems

c. Hybrid systems

1.3 GLOBAL OVERVIEW

REN21 has published its report on global energy in 2018, on which it published various data related to energy for various countries as well as globally. Following figures represent the data for global energy scenario.

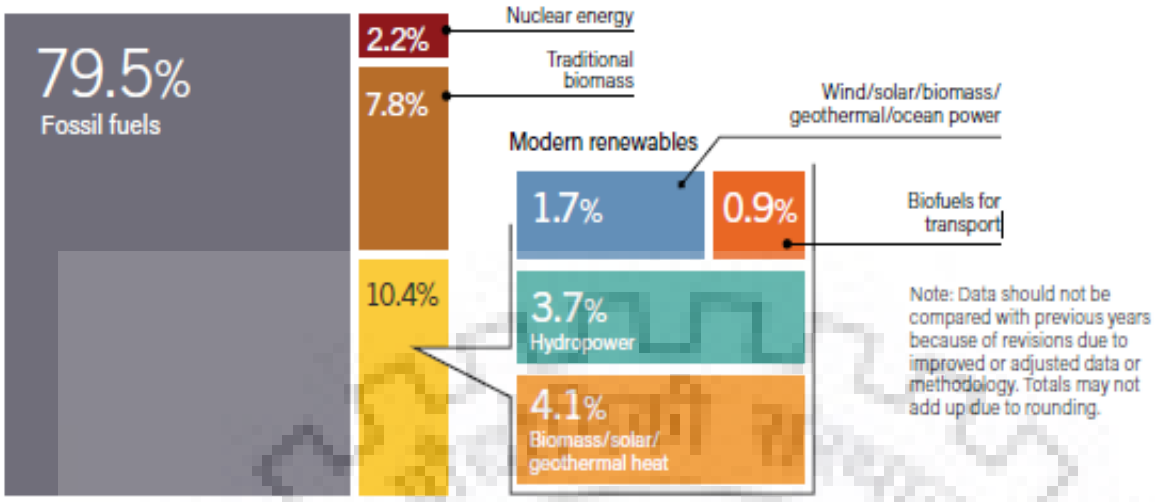

Fig. 1.2: Estimated Renewable Energy Share of Total Final Energy Consumption [2].

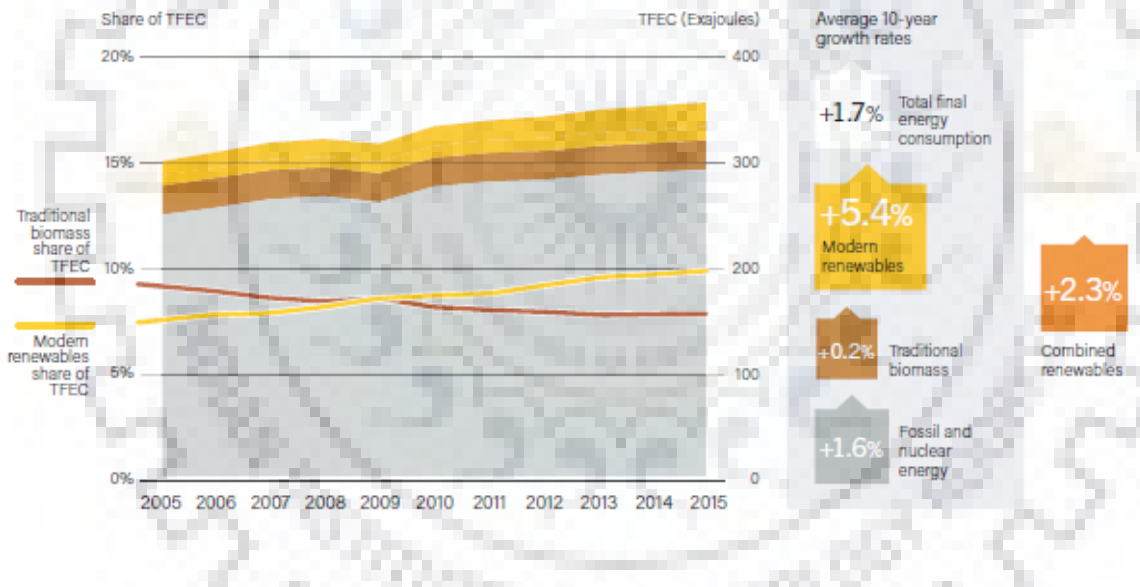

Fig. 1.3: Growth in Global Renewable Energy Compared to Total Final Energy Consumption, 2005-2015 [2].

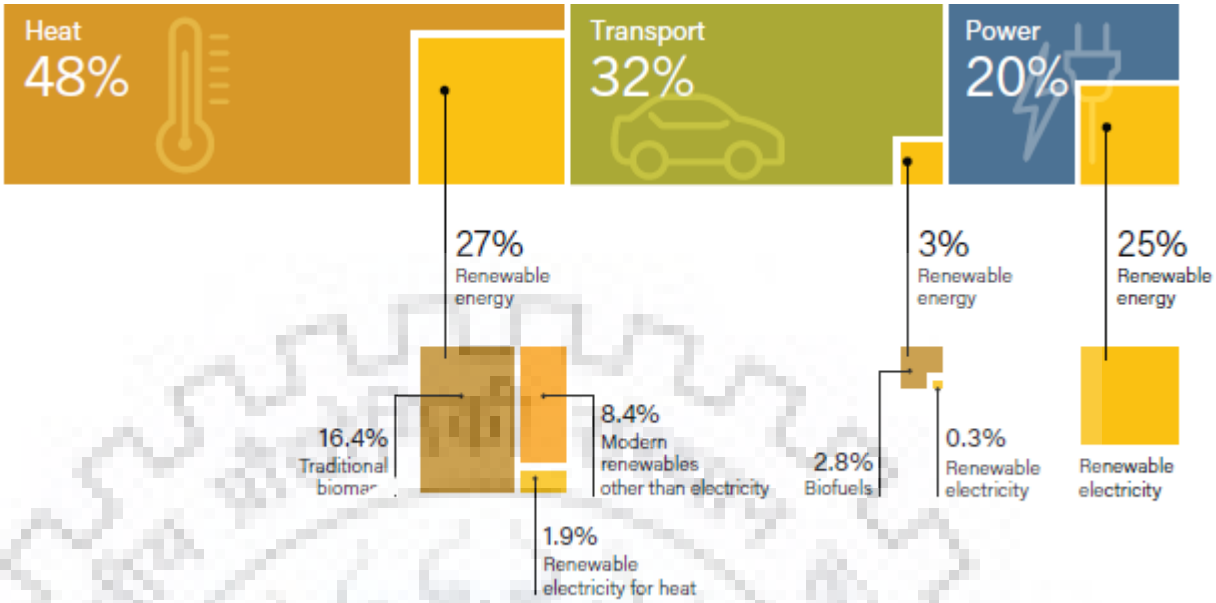

Fig. 1.4: Renewable Energy in Total Final Energy Consumption, by Sector [2].

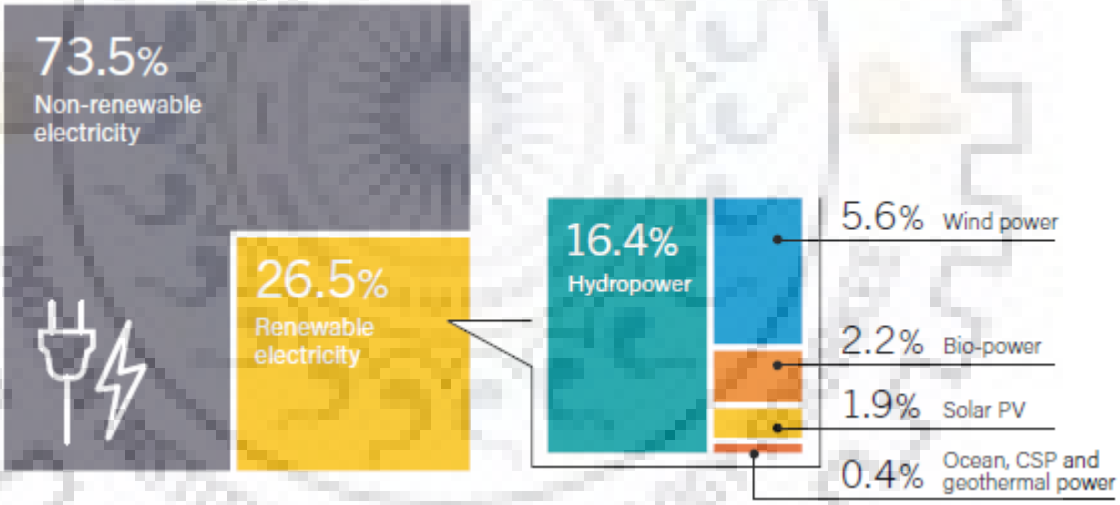

Fig. 1.5: Renewable Energy Share of Global Electricity Production, End-2017 [2].

1.3 ENERGY SCENARIO IN INDIA

The significance of electricity as a prime mover of growth is very well known and in order to improve the development of power system, the Indian Government has done the work intensely by creating various corporations namely National Thermal Power Corporation (NTPC), National Hydro Electric Power Corporation (NHPC), State Electricity Boards (SEB), and Power Grid

Corporation Limited (PGCL) etc. However, even after making this kind of effort, the country is facing power shortage in terms of energy as well as peak demand by 10.9 and 13.8 % respectively.

The power sector of India is, one of the most differentiated power sectors in the world. Sources for power generation vary from commercial sources like coal, lignite, natural gas, oil, hydro and nuclear power to other viable nonconventional sources wind, solar and agriculture and domestic waste.

1.5 CLASSIFICATION OF SOLAR ENERGY TECHNOLOGY BASED ON APPLICATION

On the basis of application solar energy can be classified as:

1. Solar thermal technology.
    a. Water heating.
    b. Solar process heating.
    c. Cooking.
    d. Solar thermal power plants.
2. Solar photovoltaic technology.
    a. Rooftop solar systems.
    b. Standalone solar systems.
    c. Grid connected solar systems.
3. Hybrid photovoltaic thermal (HPVT) technology.

1.6 HPVT SYSTEM

Solar energy can generate electricity using solar photovoltaic systems and can provide thermal load by using flat plate collectors, parabolic troughs etc. Solar energy technology is growing rapidly and is promising to the energy demands. Electricity generation and heat generation are both separate technologies of solar energy. However, recently researches are conducted on a hybrid system which is known as hybrid solar photovoltaic thermal collector. A photovoltaic thermal (PVT) collector is a solar collector which combines the thermal collectors and the photovoltaic (PV) modules to produce both heat and electricity simultaneously. Advantage of this technology is that it decreases the cell temperature which increases the cell efficiency and the hot fluid can be further used for domestic and industrial applications. The energy from sun can be utilized directly or indirectly in the form of solar energy. Solar energy is the light and heat coming from the sun

harnessed by using different solar devices for example solar heaters, solar photovoltaic cells, and solar thermal energy by thermal collectors. Producing electricity from the solar is not same as producing heat from solar.

Solar thermal principles are applied to produce hot fluids and photovoltaic principles are applied to produce electricity. Among various other renewable energy sources, potential of solar energy is highest. Solar energy has experienced the remarkable growth in recent few years due to both technological improvements and government policies which supports the renewable energy development and utilization in India and world as well. The kind of heat exchangers which convert the radiations from the sun into thermal energy by using a transport medium/fluid are solar thermal energy collectors. Photovoltaic cells utilize the solar energy and convert it into electricity by the use of photo voltaic effect. However, in today's time a new era has appeared by combining the both methods to convert energy known as "Photo Thermo Conversion". The solar energy conversion into heat and electricity with a single way called hybrid photovoltaic thermal collector (PVT) is shown in Fig. 1.6.

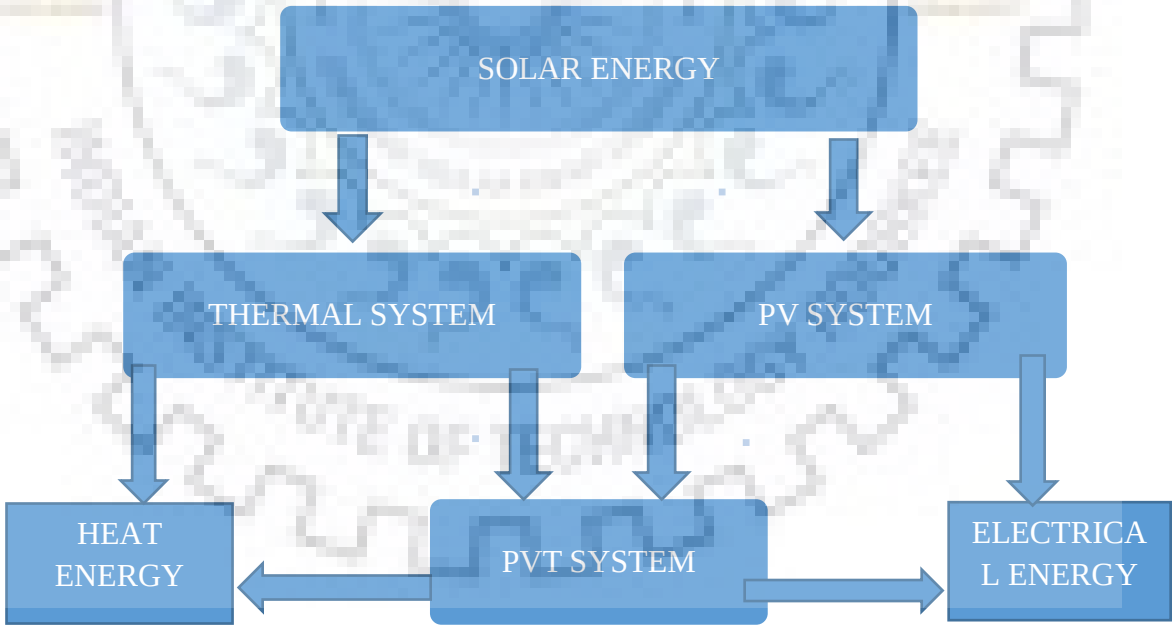

Fig. 1.6: Solar Energy Conversion in Hybrid System.

1.7 CONCEPT BEHIND PHOTOVOLTAIC-THERMAL SYSTEMS

A photo-voltaic thermal collector is a device in which the photovoltaic module is not only producing electricity but also act as a thermal absorber. So this device is producing power and heat simultaneously. The double function performed by the technology results in better overall solar conversion rate than that of just using PV or solar collector, and thus it provides a more effective use of solar energy. The solar heat and solar electricity are frequently in demand, so it's a reasonable idea to build a device like that which can conform to both the demands. Photovoltaic (PV) cells make use of a fraction of the incoming solar radiation to produce electricity and the rest becomes mainly waste heat in the cells and raises the temperature of cells as a result, the electrical efficiency of the photovoltaic module decreases, which is shown in Fig. 1.7.

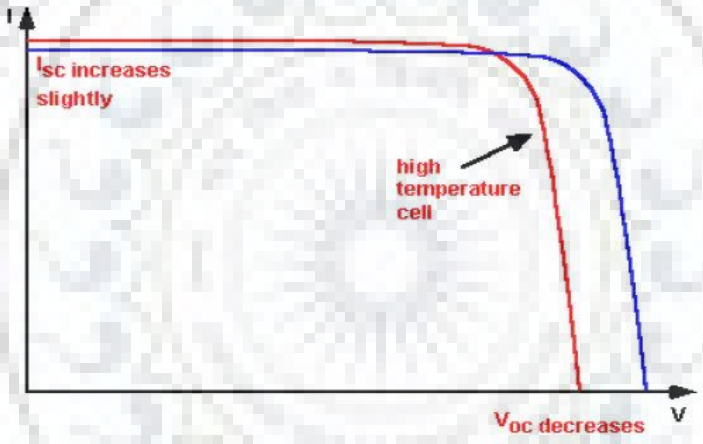

Fig. 1.7: Effect of Cell Temperature on Characteristics of PV System [3].

The photovoltaic thermal (PVT) technology recuperates portion of this heat and uses it for practical applications. The PV module gets simultaneous cooling from the transport fluid which maintains the electrical efficiency at reasonable level and thus the device make use of the solar energy efficiently.

There are different methodologies in the integration of PVT systems. Among many others, there can be selections among cooling fluid such as air, water or evaporative collectors, use of monocrystalline /polycrystalline/amorphous silicon solar cells, design criterion such as flat plate or concentrator types, type of flow such as natural or forced fluid flow, standalone or building integrated features. As it can be seen that input to the system is solar radiations by the sun and the

energy supplied to run the blower. The output is electricity generated and the thermal load which is the heat gained by the air while passing through the duct. The input and output for the PVT system can be analyzed by Fig. 1.8.

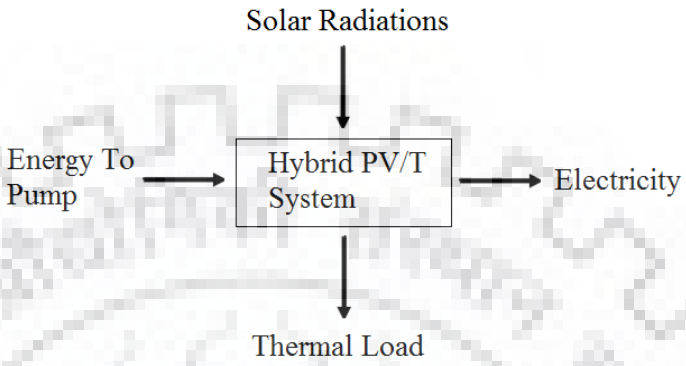

Fig. 1.8: Input and Output for a Hybrid PVT System.

1.8 TYPES OF PVT SYSTEMS

PVT systems are classified on the basis of fluid used for carrying the heat. So the two types of PVT system are given as:

1.8.1 Air PVT Collector

In practical applications of PVT systems, both water and air has been used as a cooling fluid which made PVT water and PVT air heating systems respectively. Among the PVT/Water and PVT/Air system, the former one is more efficient than the later one due to better thermo physical properties of water as compared to air. However, due to the low construction and perating cost of air based PVT system, it is utilized in many practical applications.

In air PVT collector air collects the heat from the module, which is being heated by the solar radiations. Heat collected by the air can be further used in domestic applications such as agricultural product drying, space heating. It has easy maintenance, construction and low cost as compared to water PVT collector. Fig. 1.9 shows the schematic of air PVT Collector.

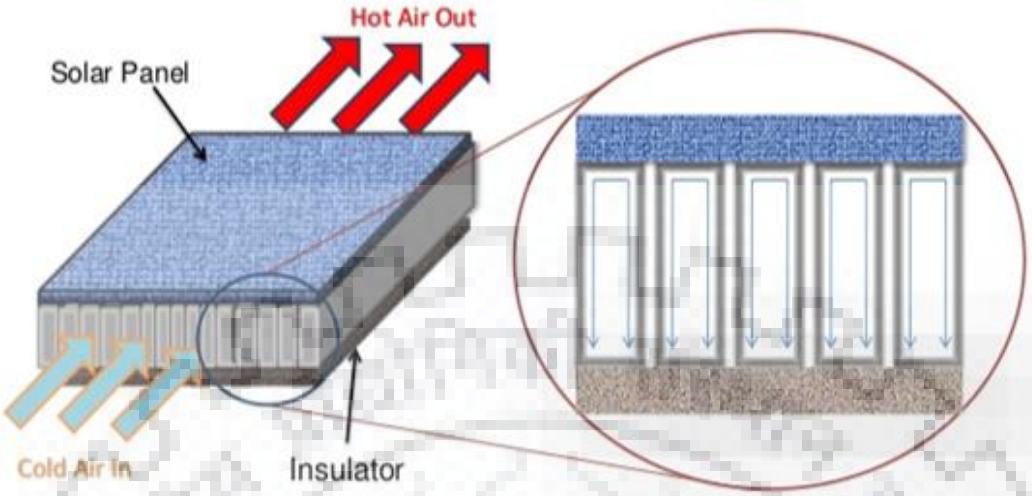

Fig. 1.9: Air PVT Collector [4].

1.8.2 Liquid PVT Collector

Liquid photovoltaic thermal (PVT) collectors are similar to the flat plate thermal collector water heating systems as both are used to heat the water and on the other hand it also generates electricity for various domestic and industrial applications. There is a parallel connection of flat plate collectors in the generally used domestic water heaters and runs on the thermo siphon action of water and there is series connection of a number of flat plate collectors in the industrial water heating systems and flow is maintained by using the photovoltaic driven pump. The material generally used as an absorber in liquid flat-plate PVT collectors is metallic sheet-and-tube absorber, while sometimes copolymer absorber is also used. The schematic of liquid PVT Collector is shown in Fig. 1.10.

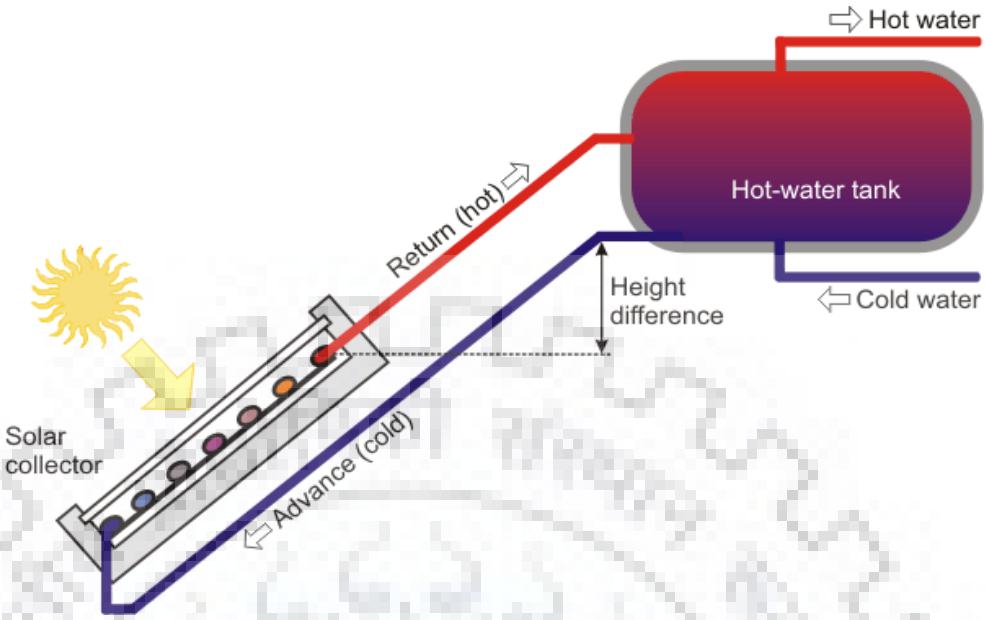

Fig. 1.10: Liquid PVT Collector [4].

1.9 ORGANISATION OF THE DISSERTATION

The dissertation work has been organized into five chapters and each chapter is presented subsequently as follows:

Chapter 1 presents the general introduction of energy and its types, global energy scenario of energy consumption and electricity production. In addition to this solar energy applications are also discussed. Further different types of hybrid photovoltaic thermal systems are also explained in this chapter.

Chapter 2 covers the extensive literature review based on solar thermal systems, solar photovoltaic systems and hybrid PVT systems. Based on the literature review gaps have been identified and finally the objectives have been set under this chapter.

Chapter 3 presents the designing details of hybrid PVT system which includes thermal, electrical and mechanical specification of the system. Different modified designs of the HPVT system are also shown in this chapter. Further introduction of CFD, meshing, solver setup, boundary conditions and calculations are also done in the later part of this chapter.

Chapter 4 covers the performance analysis of modified systems on CFD and comparison among all modified and basic systems. Final results and discussion over those results is also carried out in this chapter.

Chapter 5 concludes with the major findings and recommendations.

CHAPTER 2
LITERATURE REVIEW

Saini and Verma [5] worked for correlation between Heat transfer and friction factor for a duct having artificial dimple-shaped roughness for solar air heaters. They found that by the use of some artificial roughness (particularly spherical protrusions in their case) on the bottomside of the absorber plate of a solar air heater duct, heat transfer coefficient between the absorber plate and air can be improved by a considerable amount. They covered a range of Reynolds number (Re) between 2000 to 12,000, relative roughness height (e/D) between 0.018 to 0.037 and relative pitch (p/e) from 8 to 12. Finally they developed some functional relationships for friction factor and the Nusselt number, which is given by the equations 2.1 and 2.2 as given below.

$$Nu = f_n\left(Re, \frac{p}{e}, \frac{e}{D}\right) \quad (2.1)$$

$$f_r = f_n\left(Re, \frac{p}{e}, \frac{e}{D}\right) \quad (2.2)$$

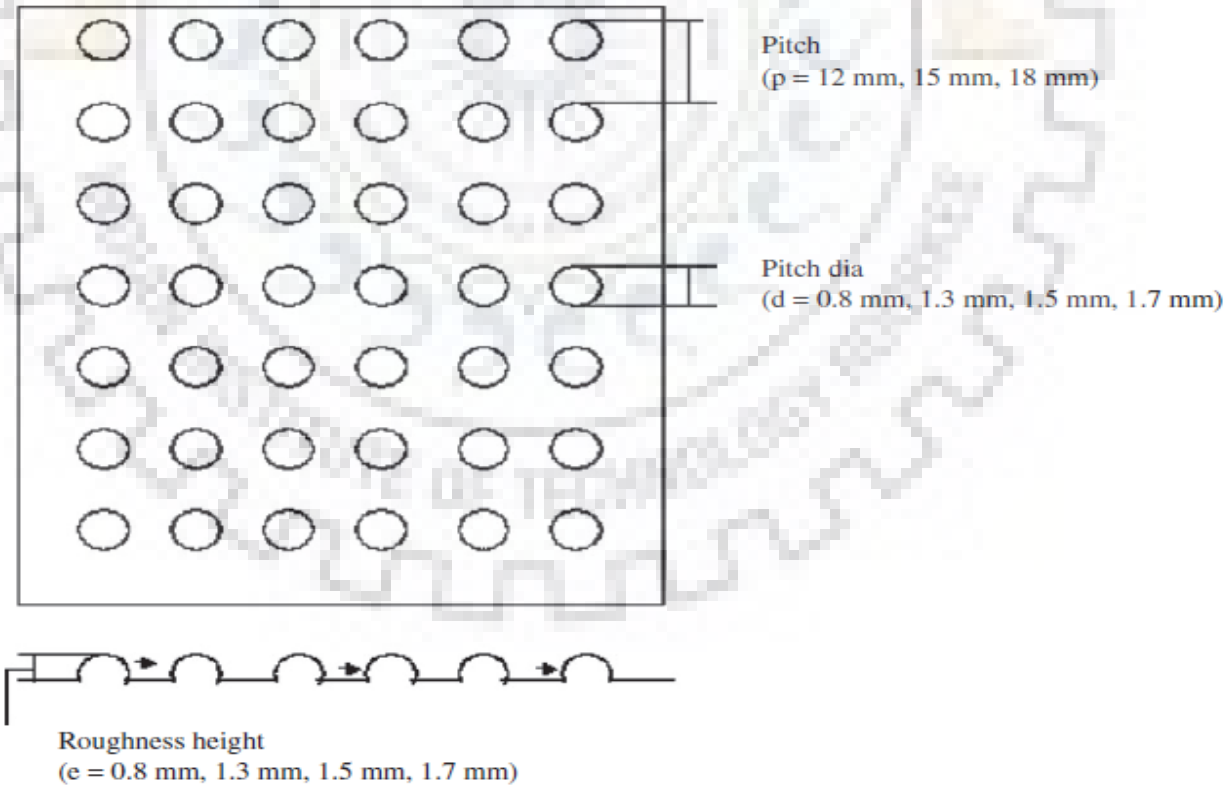

Fig. 2.1: Schematic Diagram of Dimple-Shape Geometry [1].

Based upon their experimental data, they determined the values of Nusselt number (Nu) and friction factor (fr) for different values of operating parameters and roughness, which are given below as in equation 2.3 and equation 2.4.

$$Nu = 5.2 \times 10^{-4} Re^{1.27} \left(\frac{p}{e}\right)^{3.15} \times \left[\exp(-2.12)\left(\log\left(\frac{p}{e}\right)\right)^2\right] \left(\frac{e}{D}\right)^{0.033} \times \left[\exp(-1.30)\left(\log\left(\frac{e}{D}\right)\right)^2\right] \quad (2.3)$$

$$f_r = 0.642\, Re^{-0.423} \left(\frac{p}{e}\right)^{-0.465} \left[\exp(0.054)\left(\log\left(\frac{p}{e}\right)\right)^2\right] \times \left(\frac{e}{D}\right)^{-0.0214} \left[\exp(0.840)\left(\log\left(\frac{e}{D}\right)\right)^2\right] \quad (2.4)$$

They concluded that friction factor and Nusselt number are the strong function of the system parameters and operating parameters. Maximum value of Nusselt number has been found corresponding to relative roughness height (i.e. e/D) of 0.0379 and relative pitch (i.e. p/e) of 10. While the minimum value of friction factor has been found corresponding to relative roughness height (e/D) of 0.0289 and relative pitch (p/e) of 10.

Catalin George et al. [6] worked upon the different angles of ribs which were used on panel for analysing the effect on operating temperature of solar P-V panel, and he found that it reaches about 56 °C, if no ribs are used and the maximum produced power is about 86% of the nominal power. While using the heat sink, even for short heights of ribs, the average temperature of the P-V panel was decreasing. According to simulations, the temperature was reduced by an amount of at least 10 °C below the value obtained in the basic case. This aspect is favourable for the conversion efficiency, determining a maximum power produced above 90% of the nominal power. For the configuration studied by him, the raise of maximum power produced by photovoltaic panel was from 6.97% to 7.55% comparing to the basic case, for angles of the ribs from 90° to 45° respectively.

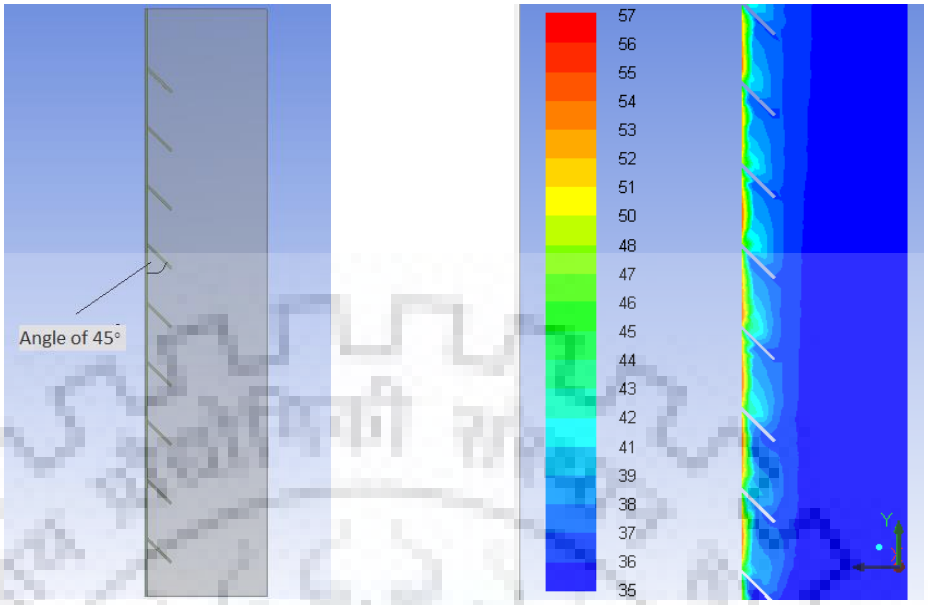

Fig. 2.2: Temperature Spectra for Rib Angle 45° and its Influence on Heat Transfer [6].

Khurana [7] attempted to conduct an experimental study in order to compare performance of a standard photovoltaic module with that of a hybrid solar photovoltaic module. In order to conduct the experimental study an experimental setup has been fabricated and solar radiations are simulated by constructing a filament box with halogen lights. Air is used as the heat transfer fluid. Experiments are conducted by varying the mass flow rate of air through the valve provided on the blower and characteristics of the photovoltaic module has been noted. Flow diagram of the experimental setup can be seen in Fig. 2.3.

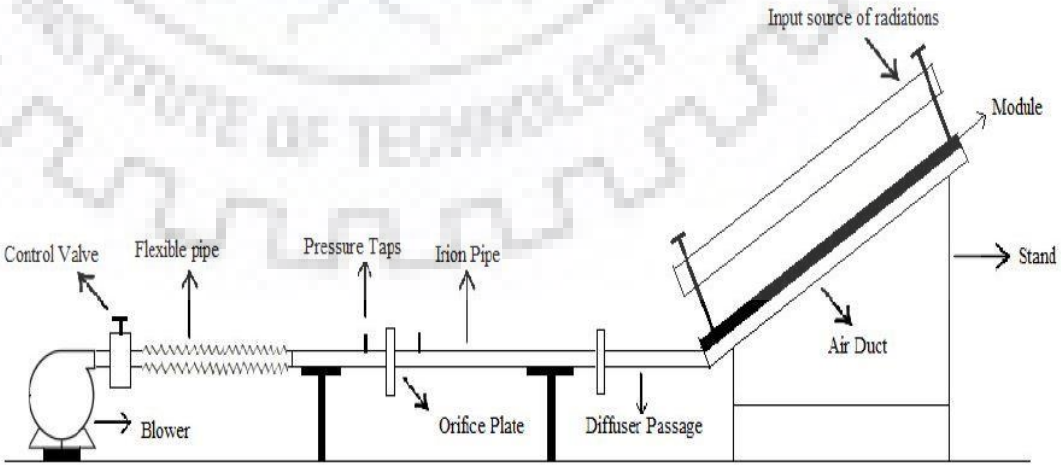

Fig. 2.3: Flow Diagram of the Experimental Setup [7].

He found that by increasing the mass flow rate of air, the net percentage gain in efficiency of the module was approximately 5% compared to the conventional PV module. This technology is very promising, his work can be concluded as:

i. A standard P-V module was used in his experimental setup, filament elements were febricated for providing simulated radiations and an air duct were designe. An experimental study was conducted to verify the effectiveness of air duct underneath the PV module and to enhance the efficiency of module.

ii. Based on his experiment study, it has been found that a maximum reduction in the module operating temperature of the order of 7˚C was achieved to increase the power output of the module. Under the reduction of temperature an enhancement of 6% in module power output has been obtained.

iii. The improved efficiency of the module with passage of air through the duct has been observed as 9.6% against the 8.8% efficiency of the module without passing air through duct. Net increment in the efficiency has been found as 5%.

iv. Based on his experiment, it has been found that there is an increase of 1.5˚C to 2˚C temperature of air passing through the duct from inlet to outlet.

A suitable improvement in power output and efficiency of PV module can be obtained by using the hybrid solar Photovoltaic Thermal collector. Based on the experimental study done, he recommended that Further net energy gain can be estimated by considering the energy supplied to blower, energy required to provide radiations, electricity generated and the thermal load available.

Mohd [8] carried out an experimental study and found that the increment in temperature is faster when water was used as heat transferring fluid as compared to oil as heat transferring fluid. The temperature variations were also observed with respect to different volume flow rate of HTFs. It was found out that increment at low flow rate was higher due to more contact time of HTF with the storage materials. The temperature is found to be decreased first along the axis but at the bottom part it again start increasing due to storage of HTF in the lower plenum. Beside this, different properties like Nusselt number, Reynolds number, Friction factor, Pressure drop across bed, Amount of Energy stored and the efficiency of storage tank has been computed. The schematic diagram of the double pass air heater is shown in Fig. 2.4.

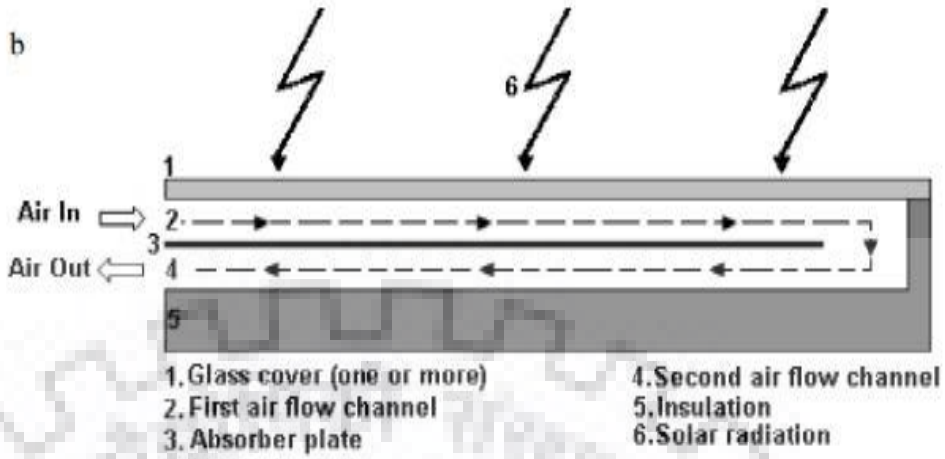

Fig. 2.4: Schematic View of Single Flow Double Pass [8].

Tiwari [9] carried out an experimental study and found that the increment in temperature is faster when water was used as heat transferring fluid as compared to oil as heat transferring fluid. The temperature variations were also observed with respect to different volume flow rate of HTFs. It was found out that increment at low flow rate was higher due to more contact time of HTF with the storage materials. The temperature is found to be decreased first along the axis but at the bottom part it again start increasing due to storage of HTF in the lower plenum. Beside this, different properties like Nusselt number, Reynolds number, Friction factor, Pressure drop across bed, Amount of Energy stored and the efficiency of storage tank has been computed. He recommended that more investigations are required to determine the pumping power needed in the system in order to find out the net gain in storage efficiency.

Bhargava et al. [10] analysed the grouping of photovoltaic system and an air heater. Calculations are done on the different configurations of the air heater to find out the optimum area of the photovoltaic cells required to generate the necessary electrical energy for the pump. It was found that with the increase of mass flow rate and fraction of area covered by photovoltaic cells, air heater efficiency increases.

Bergene [11] proposed algorithms for the creation of quantitative predictions regarding the performance of the detailed physical model of hybrid PVT system. Energy transfer analysis was the

basis of model. The model predicts the performance of the system fairly well with system efficiencies, thermal +electrical, about 60-80%.

Sopian et al. [12] analyzed the performance of single-pass and double-pass combined photovoltaic thermal collectors with steady-state models and taking air as the working fluid. Two types of combined photovoltaic thermal collectors are compared. Based on the results it was found that double pass photovoltaic thermal collector has better performance.

Tonui and Tripanagnostopoulos [13] studied the natural flow of air as a cooling medium in the commercial PV module made as PVT air solar collector. The methods which are considered consist of thin metal sheet hanging at the middle or attachment of fins to the back wall of the channel of air so that heat extraction from the module can be improved. They analyzed effect of incident radiation, channel depth and collector length on thermal and electrical efficiencies.

Ibrahim et al. [14] presented the classification of flat plate PVT collectors, performance estimation of water, air and the combination of water and/or air PVT system. The easy to manufacture and simple in construction design of the system was concluded to be tube and sheet design, even though, its efficiency is 2% inferior compared to other types of collectors for example, free flow, channel type and two-absorber type.

Aste et al. [15] analysed several researches carried out on flat plate PVT water collectors and their components. He concluded that in order to increase the thermal energy, in the range of 10–30%, a top cover may be adopted, however such cover decreases the electrical output in the range of 1–10%, depending on the transmission factor of the cover.

Sharma et al. [16] developed a CFD model of solar air heater with artificial roughness of square type protrusion. Reynolds numbers taken for the study were in between 4000 to 20000 and relative roughness pitch of 38.8-61.1 at fixed relative roughness height of 0.016mm. Correlation was developed for Nusselt number and friction factor utilizing the results obtained by CFD model.

Makki et al. [17] studied and employed various methods to attain cooling action for PV systems. Discussions were carried out regarding the designs employing liquid, air, PCM, heat pipe

and thermo electric modules to support cooling of PV cells along with the influence of parameters on the system performance.

Takashima [18] evaluated the energies obtained from the PVT panel such as thermal and electric energies. Solar cell temperature increases up to the suggested temperature of thermal energy use. The method was proposed to not to decrease the cell conversion efficiency based on the evaluation done. Having a gap between the solar panel and the collector improves the performance of PVT system as compared to the conventional PVT system.

Gunter et al. [19] investigated thermoelectric cogeneration solar collectors and obtained two different principles. The first one is thermoelectric collector (TEC) and the other one is photovoltaic hybrid collector (PVHC). They concluded that the electrical output from the PV-hybrid collector is considerably higher than that of the thermoelectric collector.

Charalambous et al. [20] studied the parameters affecting PVT performance (electrical and thermal) and concluded that the efficiencies of PVT system could range from 60 to 70% for low quality collectors and for perfect collector respectively according to analytical and numerical models. Liquid PVT Collectors are more efficient than the air one.

Santbergen et al. [21] investigated the options to use the anti-reflecting coating and low emissivity coatings as to improve the annual electrical and thermal yield of system with PVT collectors. Application of AR coatings in the case of covered PVT collectors is quite favourable for both the annual thermal efficiency and the annual electrical efficiency. The application of a low-e coating is favourable in the case of annual thermal efficiency but it decreases the annual electrical efficiency.

Alfegi et al. [22] presented a mathematical model and solution procedure of a single pass photovoltaic thermal air collector (PVT) with fins on both sides of the absorber. The prediction of circulated air temperatures for both sides as a function of distance in the flow direction was done.

Hayakashi et al. [23] established the photovoltaic/thermal (PVT) hybrid panel with a PVT total conversion efficiency of 60% or above by combining solar cells and a solar heat collector for private houses.

Othman et al. [24] performed experiments on the system for low temperature applications. Theoretical studies were done on a finned double pass PVT solar air heater. Heat removing fluid used was air, monocrystalline silicon cells were pasted to the absorber plate having fins on the other side. They concluded that it is important to use fins as an integral part of the absorber surface.

Amaraoui and Aliane [25] conducted simulation of solar air heater on ANSYS workbench. ANSYS ICEM was used for high quality mesh generation. Solar air heater with baffles was taken for study which was placed between the insulator and the absorber. Baffles were found to serve the role of the fins and thus heat transfer was found to be increasing.

Kapardar and Sharma [26] developed a CFD model of solar air heater with and without porous media. It was concluded that porous media has significant effect on the performance of solar air heater. Higher thermal performance was found for porous media than non-porous media. Depth variation of solar air heater duct was also studied and was found to have effect on the outlet temperature of air. Outlet temperature for both porous and non-porous media was found to be decreasing with increase in depth.

Katedar et al. [27] conducted experimental investigation of solar air heater with artificial roughness. Formation of laminar sub- layer was studied and shown to have high influence over heat transfer. Considerable improvement in heat transfer coefficient was found for solar air heater with artificial roughness.

The summary of important works related to this dissertation work is given in Table 2.1.

Table 2.1: Summary of important works Closely Related to the Dissertation Work.

S. No.	Title	Author(S)	Findings
1.	Heat transfer and friction factor correlations for a duct having dimple-shape artificial roughness for solar air heaters (2007).	Saini and Verma	Correlations for Nusselt number and friction factor have been established for solar air heater
2.	Efficiency improvements of pv panels by using air cooled sinks (2015).	Catalin et al.	Heat transfer was maximum at 45 degree rib angle.
3.	Experimental investigation of hybrid solar photovoltaic thermal collector (2016).	Khurana	By increasing the mass flow rate of air, the net percentage efficiency gain of the module was 5%,
4.	Study of a hybrid solar system-solar air heater combined with solar cells (1991).	Bhargava et al.	Air heater efficiency increased by increasing the mass flow rate of air.
5.	Experimental study on performance of a double pass solar air heater (2016).	Mohd. Insha	Temperature increment was more in water as compare to oil as HTF.
6.	Model calculations on a flat-plate solar heat collector with integrated solar cells (1995).	Bergene and Lovvik	Done Energy transfer analysis and predicted thermal +electrical, efficiency about 60-70%.
7.	Performance analysis of Photovoltaic Thermal air heaters (1996).	Sopian et al.	Single-pass and double-pass pvt collectors were compared and it was found that double pass pvt collector has better performance
8.	CFD based investigation on effect of roughness Element pitch on performance of artificial roughness duct used in solar air heater (2011).	Sharma et al.	Worked on artificial roughness of square type protrusion. Correlation was developed for Nusselt number and friction factor utilizing the results obtained by CFD model

2.1 GAPS IDENTIFIED

Based on the literature review, it is found that there are certain research areas which are still untouched or partially unveiled. Thus, further research work can be done in these areas to improve the performance of a hybrid photo voltaic thermal system. In brief, these gaps are summarized below.

1. work has been carried out for enhancing the electrical output of PVT system but it is found that there is almost no work is done to optimise the energy balance such as energy supplied by the pump or blower, electrical output of system, waste thermal energy by conduction, convection and radiation (although radiation losses will be negligible at lower temperature).
2. Most of the researchers have used double pass duct with water and air as a cooling fluid for increasing the heat transfer rate to improve efficiency, but the very few have used roughened ducts and ribs to analyse the heat transfer rates for increasing the output or efficiency of system. So this research area can also be explored and some improvements also required in the system for the same.
3. Many researchers have done the work to improve the efficiency of Solar PV and Solar Thermal system separately, but almost no work has been carried out for Hybrid Photo Voltaic Thermal system (HPVT), to increase its efficiency by changing the design of HPVT system such as, inserting the ribs at a certain angle, increasing roughness of heated module, inserting inverted path or double pass, selecting suitable HTF (heat transfer fluid).

2.2 OBJECTIVES

Objectives of this dissertation work are mentioned below.

1. To find out the factors and parameters which can affect the performance of HPVT system.
2. To develop (design) a basic working model for analysis.
3. To modify the basic working model using those factors and parameters which affect the performance of HPVT system.
4. To analyse and compare the results of basic and modified system.

2.3 METHODOLOGY ADOPTED

Various steps followed during this dissertation work to reach the desired objectives are listed below.

1. Identification of gaps after literature review.
2. Design of basic working model for analysis.
3. Selection of suitable method among experimental, analytical and computational method for analysis.
4. Finding out the factors and parameters which can affect the performance of HPVT system by analysing the system with the help of different theories related to heat transfer and fluid mechanics.
5. With the help of these parameters, efficient and modified working models are developed on a designing software (solid works).
6. These basic and modified designs are imported on CFD software for their performance analysis.
7. After the analysis of the basic system and modified system, three types of efficiencies (photovoltaic, thermal and system efficiencies) are calculated for all the systems.
8. Finally the comparison of results is done for simple and modified systems, and the most efficient way to design HPVT system is proposed.
9. Documentation and submission of dissertation report.

Proposed method can be better understood with the help of following flowchart shown below in Fig. 2.5.

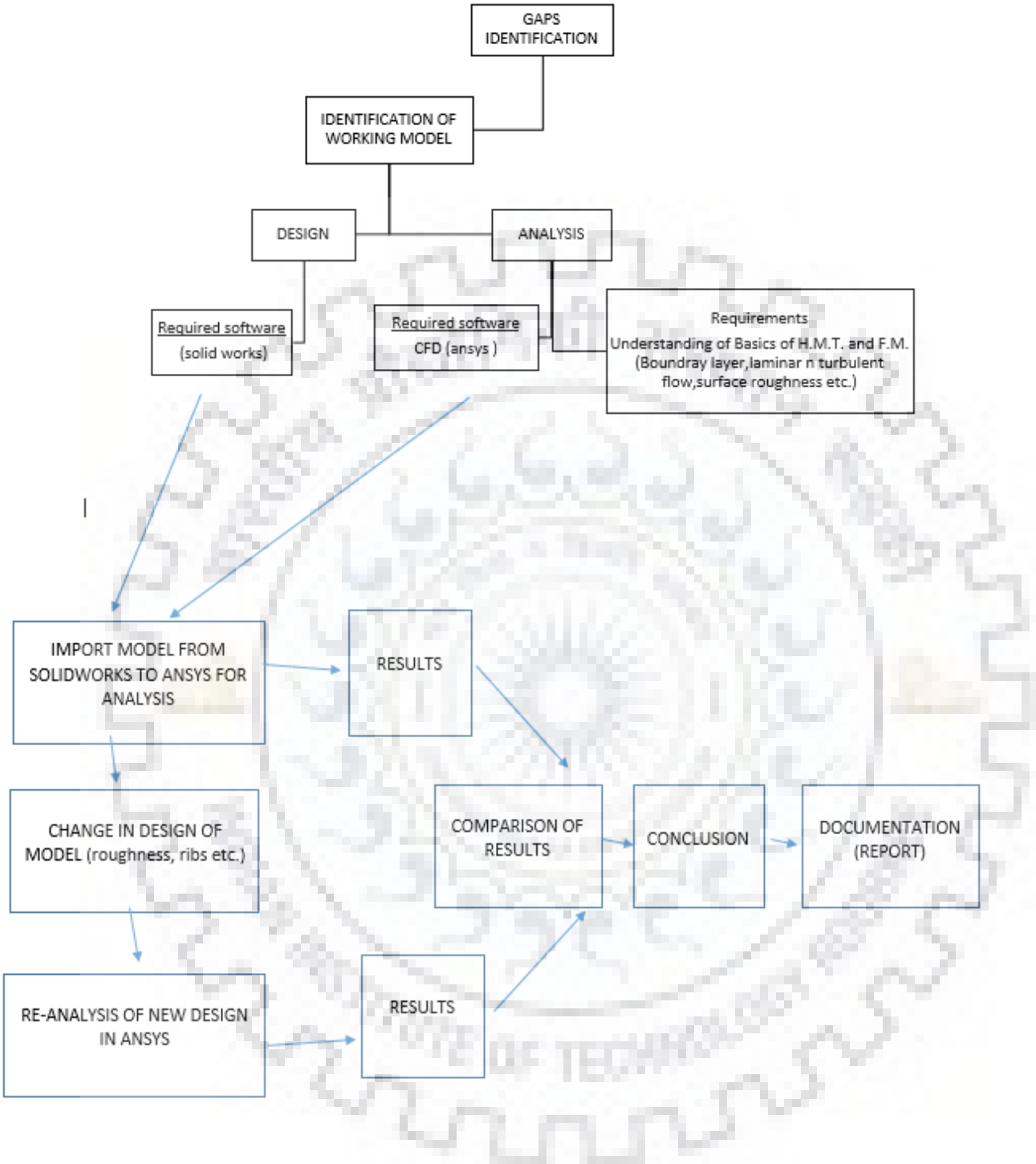

Fig. 2.5: Flow Chart for Methodology Followed.

CHAPTER 3
DESIGNING DETAILS OF HPVT SYSTEM

3.1 GENERAL

Under this dissertation work, HPVT system is taken into consideration by making a basic model. In the model a simple duct is placed beneath the absorber plate, which is attached to the heated panel for taking the heat from the heated panel. When the heat transfer fluid (HTF) is passed through the duct, it carries away the heat from absorber plate hence the temperature of absorber plate and panel get reduced, which finally increases the performance of HPVT system. The schematic of the basic working model of HPVT system is shown in Fig. 3.1.

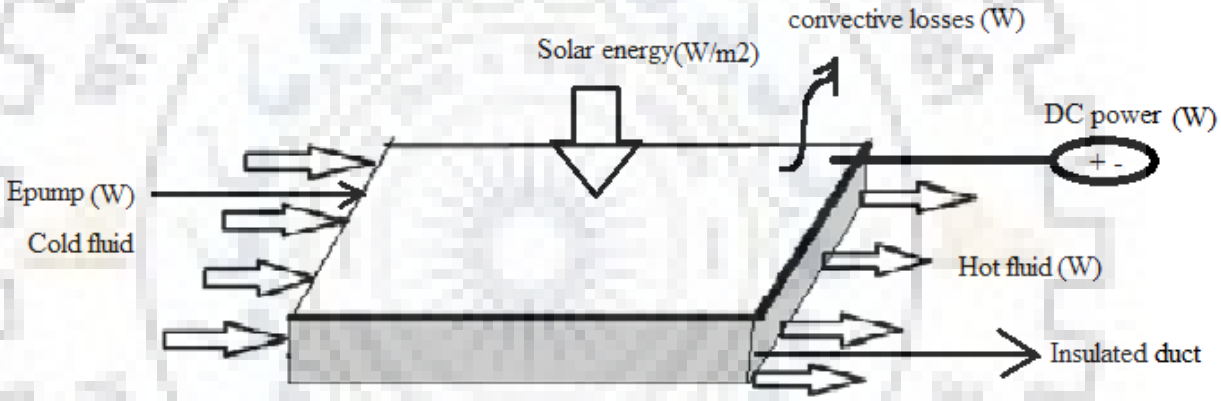

Fig. 3.1: Schematic of Working Model.

3.1.1 Considered Assumptions for Analysis

Following assumptions are considered for the analysis of basic system.

1. Losses through duct are neglected (perfect insulation).
2. Radiation losses are neglected.
3. Steady state analysis.
4. Volumetric energy generation is neglected, i.e., $E_{gen} = 0$
5. Total heat absorbed by solar panel is transferred into the absorber plate, placed below the heated panel and convection loss which is taking place only from the top surface of solar panel.

So, after considering these assumptions energy equation can be written as:

$$E_{in} + E_{gen} = E_{out} + \text{losses} \quad (3.1)$$

Or, $E_{in} = E_{out} + \text{losses}$ (3.2)

Therefore by putting the values of E_{in} and $E_{out,}$ equation 3.2 can be written as:

$$E_s + E_p = E_e + E_f + \text{Convection Losses} \quad (3.3)$$

Where,

Es is the solar energy absorbed by panel in Watt,

Ep is energy required to drive the pump in Watt,

Ee is electrical power generated by panel in Watt,

And E_f is energy carried away by fluid in Watt.

Here in the above equation 3.3, it can be analyzed that;

(i). Es depends upon location and it is fixed for a particular location, so it is considered as a constant for present analysis.

(ii). Ep should be optimized, but it is fixed for a particular mass flow rate, so it is also not the area of interest for present work.

(iii). Ee is constant for a particular panel at a given temperature, so it can't be changed without changing the panel temperature, therefore it can also be considered as a constant for a given panel temperature.

(iv). E_f (Energy carried away by fluid) is the only energy, that can be affected by altering the design. This is the energy on which this dissertation work is mainly focused and several modification are done to maximize this E_f .

So, for that purpose, parameters must be known which affect the heat transfer rate. These parameters can be understood with the help of some basic concepts of heat transfer and fluid mechanics, and also with the help of some earlier research work, which carried out on those parameters which increases the heat transfer rate of solar air heater and other thermal devises.

3.2 FACTORS CONTRIBUTE IN HEAT TRANSFER

With the help of different researches, laws and theories, the major factors, which affect the heat transfer rate are listed below.

1. Thermal properties of heat transfer fluid (HTF) like convective coefficient (h), thermal conductivity of fluid (k_f) and specific heat (c).
2. Kinetic properties of HTF like velocity and viscosity.
3. Fins (Extended surfaces).
4. Ribs (Turbulators).

5. Design and angle of fins and ribs.
6. Type of flow (Laminar or Turbulent).
7. Artificial Surface roughness.
8. Relative pitch and roughness height.
9. Dimensionless numbers (Reynold Number, Nussult Number, Prandlt Number etc.).

Among all these factors and parameters, some of them are considered in present work for analysis to increase the heat transfer rate from absorber plate (placed below the panel) to HTF through duct. Selected methods to increase the energy gain (E_f) by fluid are as follow.

3.2.1 Inserting the Ribs/ Turbulators

The effects of inserting the ribs on the HPVT system can be understood by the following flowchart.

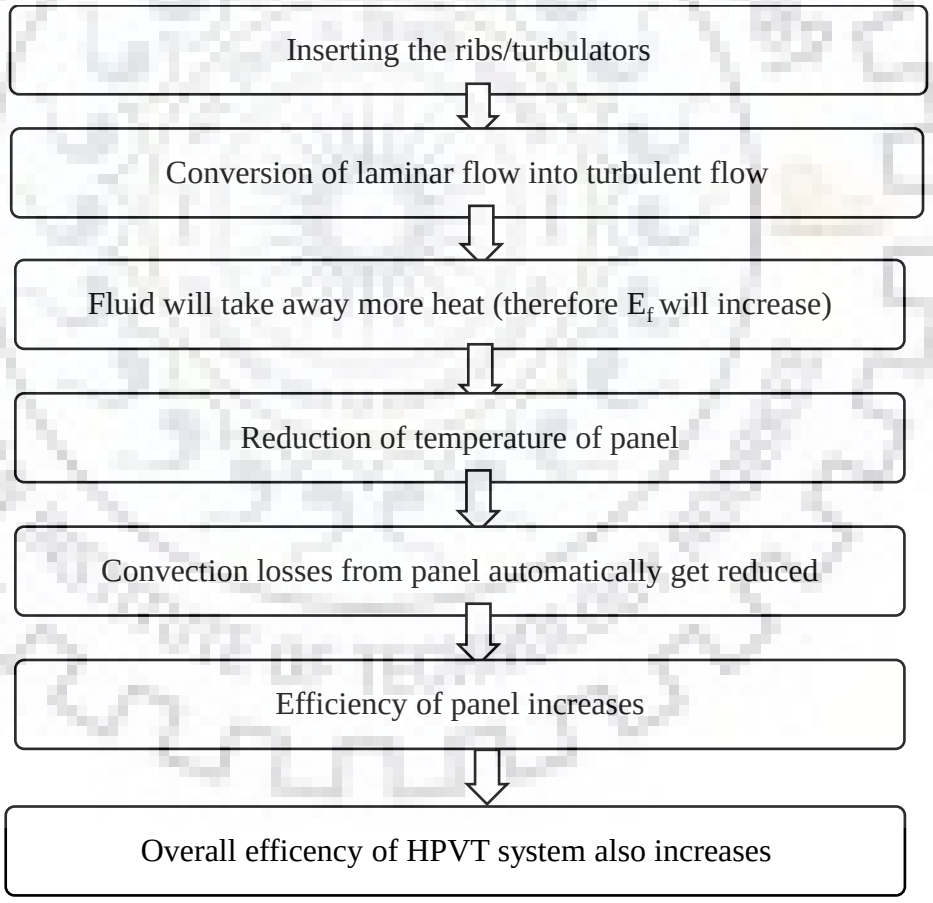

Fig. 3.2: Flowchart for Understanding the Effect of Inserting the Ribs.

3.2.2 Artificial Surface Roughness

The effect of making the surface rough can also be understood with the help of given flowchart.

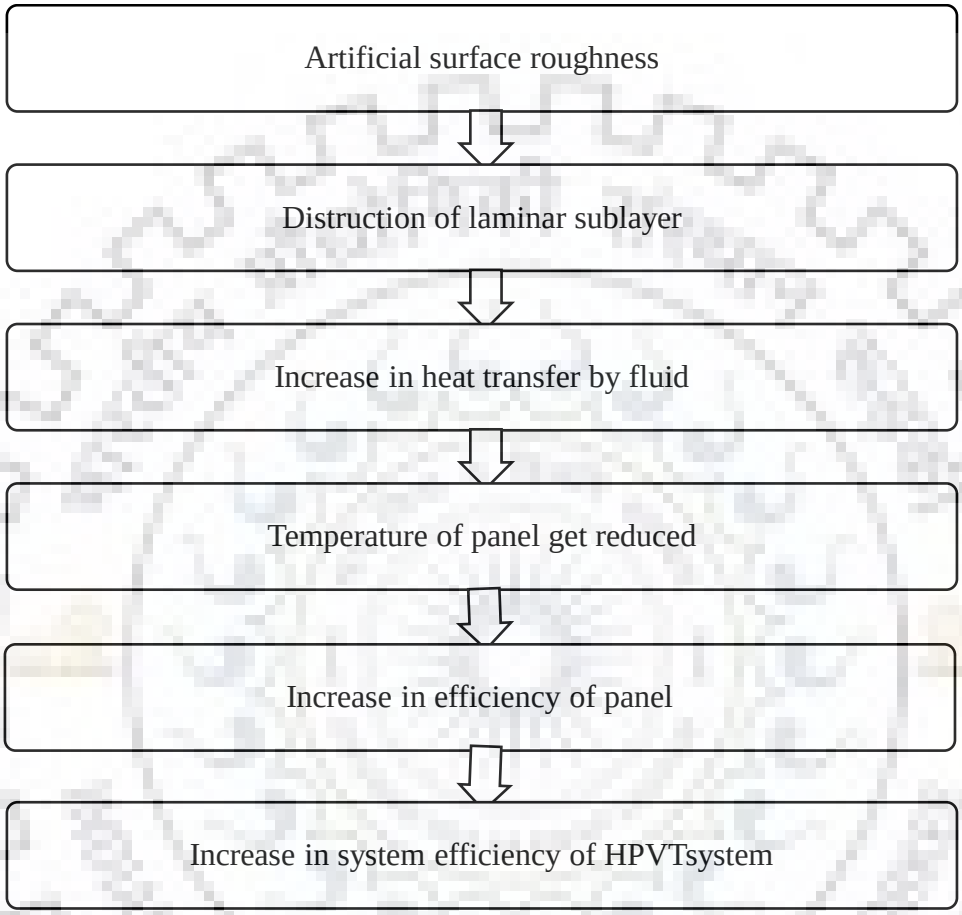

Fig. 3.3: Flowchart for Understanding the Effect of Rough Surface.

3.2.3 Selecting the Fluid with Larger K_f and h

At boundary (wall of panel), heat is transferred through conduction mode, therefore K_f must be high so that heat transfer from boundary to adjacent layer will be high as per the given equation 3.4.

$$Q = - k_f \times A \times dT/dx \qquad (3.4)$$

Where,

K_f is thermal conductivity of adjacent layer of fluid,

A is the area of conducting surface,

dT/dx is the tempertature gradient in the direction of heat flow.

From this layer of fluid heat is transferred by convection to the remaining fluid, therefore h must be high as per given equation 3.5.

$$Q = h \times A \times \Delta T \quad (3.5)$$

Where,

h is convective heat transfer coefficient of fluid,

ΔT is the temperature difference.

K_f and h are high for water as compare to air, so water is better as compare to air for increasing the heat transfer rate, but the handling, pumping and circulating of water is difficult as compare to air. In this dissertation, air is mainly used as a HTF.

3.2.4 Alteration in Angle of Rib

It is found from various researches that the ribs which are attached at an angle of 45° are more efficient in hear transfer as compare to ribs at any other angle like 90°, 135° etc. So, it can be said that varying the rib angle can enhance the heat transfer from the heated panel.

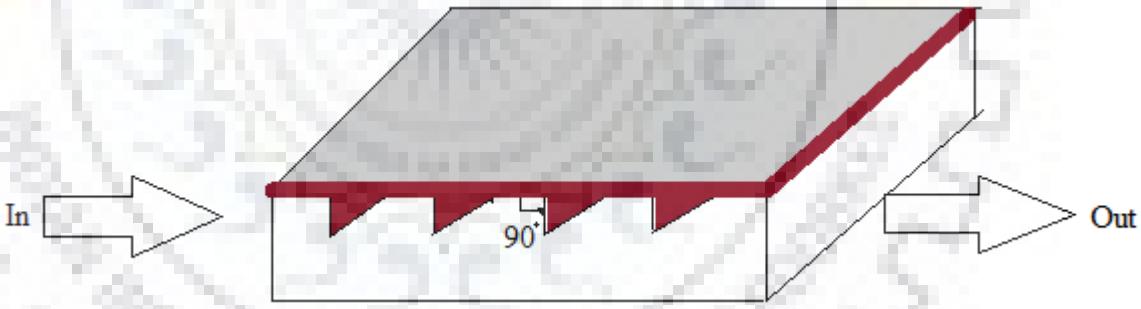

Fig. 3.4: Duct Having Ribs at 90°.

3.3 EFFICIENCY OF HPVT SYSTEM

All the earlier methods which are discussed here, are increasing the heat transfer rate from panel to HTF (heat transfer fluid), hence finally reducing the temperature of panel, and this will increase the efficiency of panel, The relation for efficiency can be written as:

$$\eta = \frac{energy\ output(W) from\ PVT\ sysyem}{energy\ input(W) to\ the\ PVT\ sysyem}$$

Or, $\eta = (Ee + Ef)/(Es + Ep)$ (3.6)

Consideration of the different efficiencies, loss is an important factor. The major convection losses from heated panel are considered in the study, which can be calculated by given equation 3.7.

Major Losses = Convective losses = $h \times A \times (Tp-Ta)$ (3.7)

Where,

h is the convective heat transfer coefficient

A is the exposed surface area of panel

Tp is panel temperature

Ta is ambient temperature

Incident solar energy falling and absorbing on the solar panel can be taken as the input energy to the system and is given in equation 3.8

Es = solar energy absorbed by panel = $(1-\rho) \times A \times I$ (3.8)

Where,

ρ is the reflectivity of panel (for analysis, $\rho = 0$)

I is the total radiation (beam+ diffused) falling on panel = 1000 W/m^2

A is the exposed area of panel

Ep is energy required to drive the pump

Ee is electrical power generated by panel

E_f is energy carried away by fluid, and given by the equation 3.9.

$E_f = h \times A \times (T_p-T_f) = m \times c \times (T_o - T_i)$ (W) (3.9)

Where,

h is convective coefficient of HTF,

T_p is the panel temperature,

T_f is local fluid temperature,

T_i is inlet fluid temperature,

T_o is outlet fluid temperature.

Here temperature of fluid (T_f) is varying continuously from inlet to outlet of insulated duct, attached to heated panel, so it cannot be calculated directly. Therefore, there is a need to select one method among computational, experimental and analytical method for calculating the value of energy interaction (E_f) and efficiencies.

The objective of obtaining the data for the performance analysis can be achieved by the following three ways, depending upon the requirements and feasibility of the method. The three ways to get the desirable objectives are:

a) Computational method
b) Experimental method
c) Analytical method

The comparison of the above methods are presented in Table 3.1.

Table 3.1: Comparison of Different Methods.

S. No.	Methods	Advantages	Disadvantages
1.	Experimental	More realistic results.	Equipment are required so high operating costs and more time taking.
2.	Analytical	Generalized results.	Calculations are complex.
3.	Computational	Easier to obtain results, time and cost saving method.	Skilled persons are required, truncation errors are there.

Under this work computational method is considered for getting the required data for analysis, and CFD analysis of basic and modified models are done on Ansys 15.0 with the following inputs to the system to get those desired data for further analysis.

3.4 INPUTS AND BOUNDRY CONDITIONS USED FOR CFD ANALYSIS

1. Temperature of heated panel- 333K.
2. Material of absorbing plate- Aluminium.
3. Dimension of duct 1.64×1×0.1 (l×b×h) in meters.
4. Wall material of insulated duct- Wood.
5. Type of heat transfer fluid- Air.
6. Reynolds number- (1200-7200).
7. Hydraulic diameter of duct– 182mm.
8. Velocity of HTF at inlet- (0.1-1.0) m/s.
9. Ambient temperature- 300K.
10. Incident solar radiation- 1000 W/m^2.

Temperature, velocity, pressure and other variations can be analyzed after providing these inputs and boundary conditions to the given basic model which is shown in Fig 3.3.

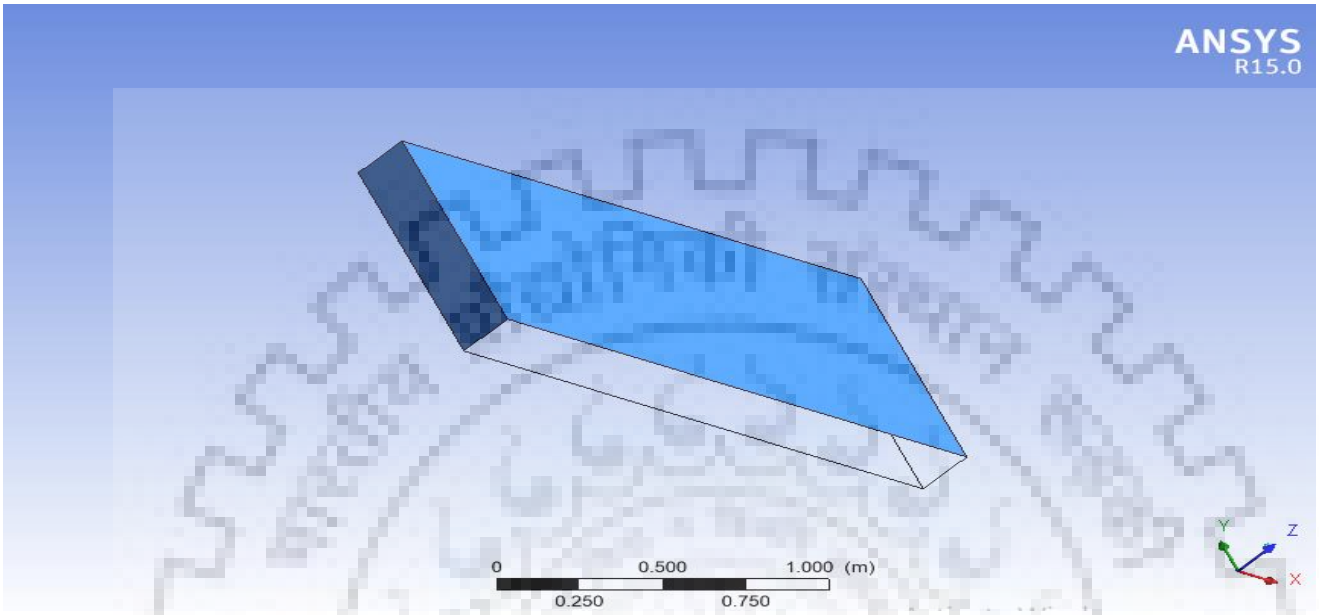

Fig. 3.5: Design of Basic Model Made in Ansys.

3.5 OUTPUT FOR BASIC MODEL

Output of the analysis can be seen in the following figure which is taken from the CFD software (ansys).

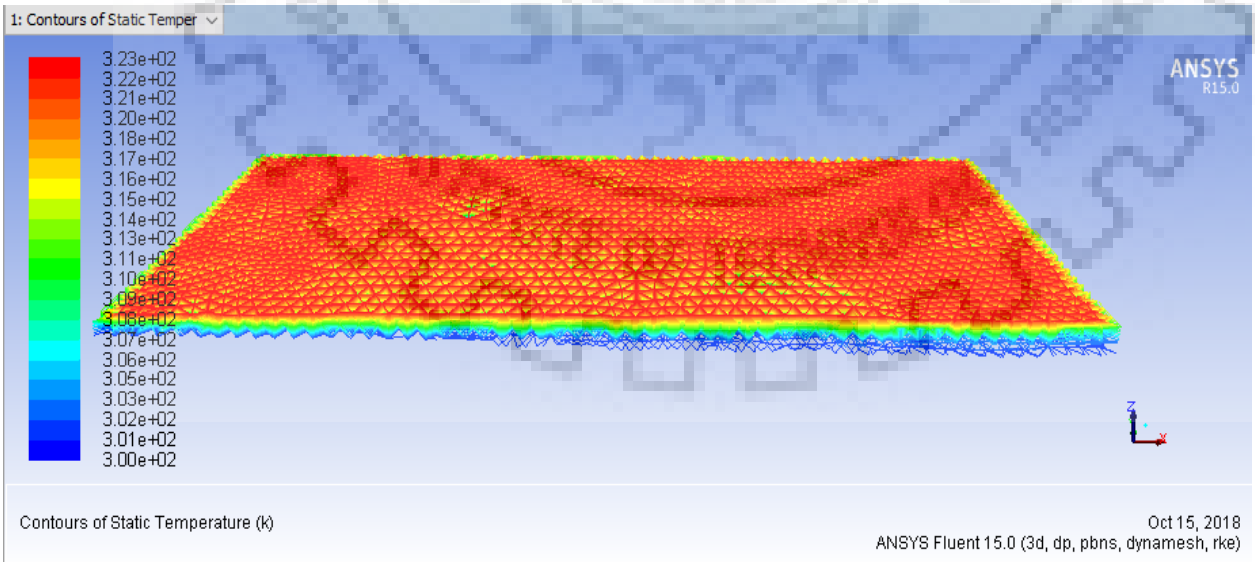

Fig. 3.6: Temperature Variation of Fluid in the Duct.

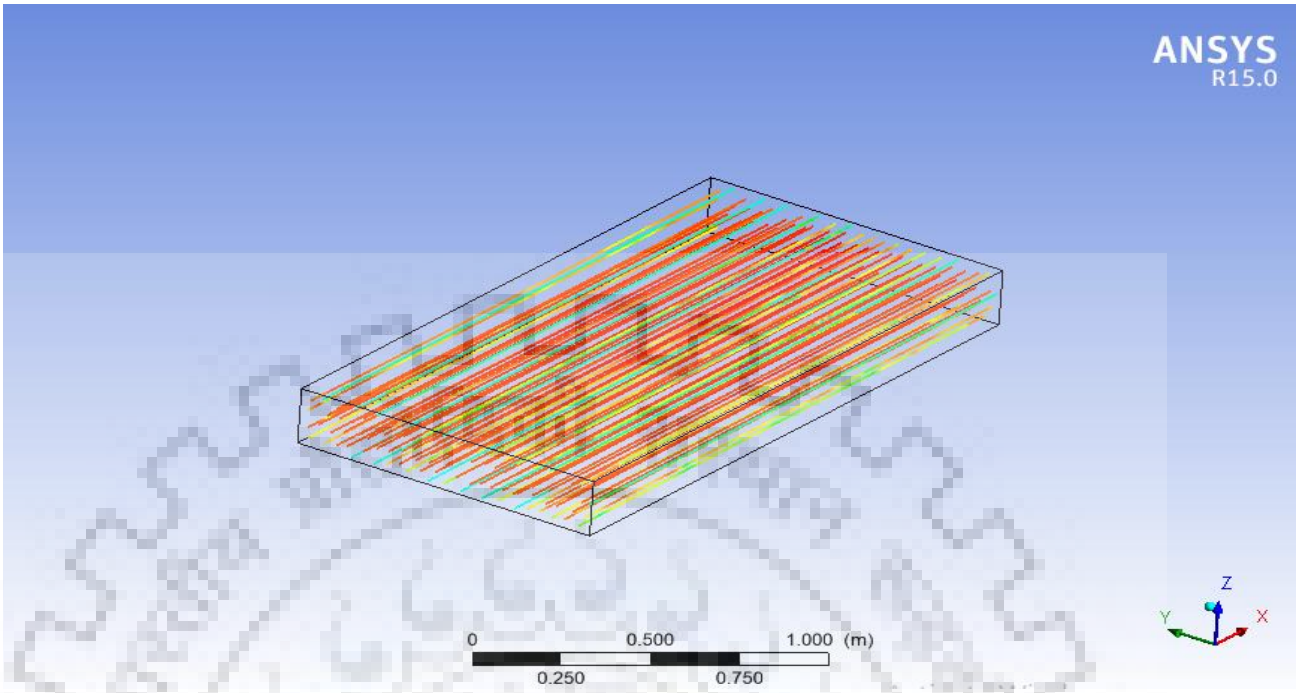

Fig. 3.7: Stream Line Reorientation of Fluid inside the Duct.

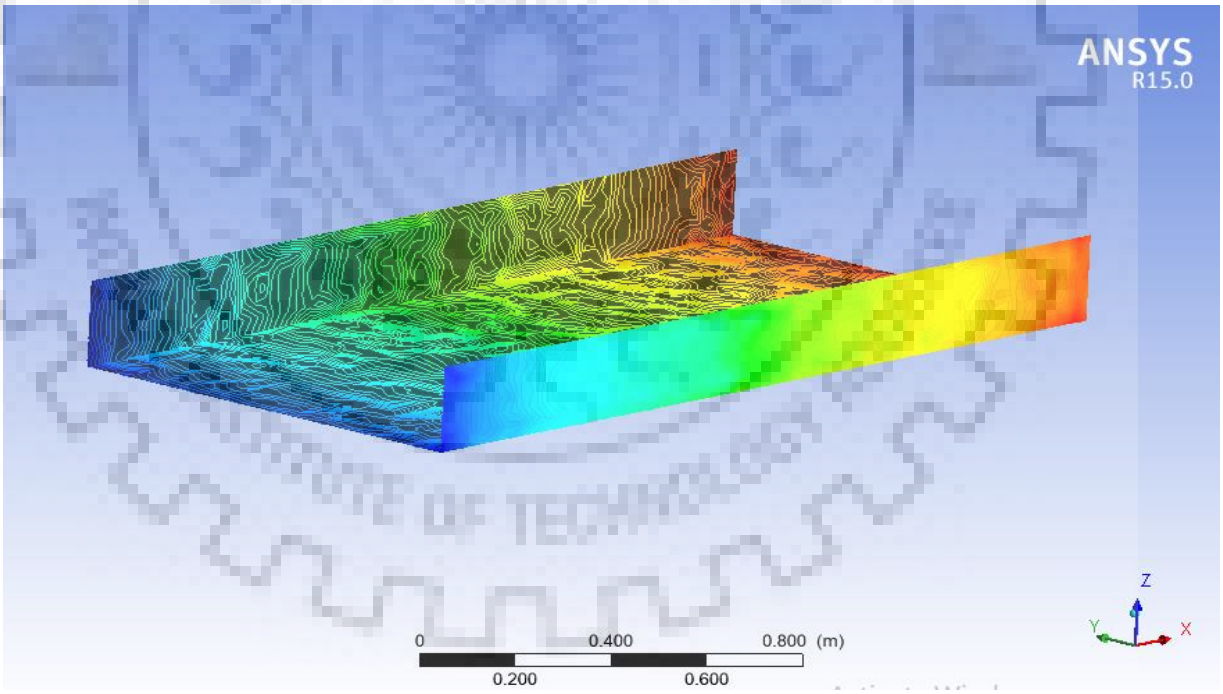

Fig. 3.8: Variation of Temperature along the Duct.

3.6 RESULTS FOR ANALYSIS OF BASIC MODEL

It can be seen that there is a minute change in temperature of incoming and outgoing fluids, which implies that air is carrying very less heat from the heated panel. Thus, there is a need for doing some modification in the design of working model, so that fluid can carry more heat from the heated panel, So that, if somehow it is possible to increase the heat transfer from heated panel to fluid, T_p (temperature of panel) reduces and following effects can be obtained on efficiency (given by equation 3.10) of PVT system.

$$\eta = (Ee+Ef) / (Es+Ep) \quad (3.10)$$

1. Reduction in panel temperature increases the E_e, which further results in increased efficiency.
2. Reduction in T_p facilitates the HTF to transfer more heat from heated panel, therefore E_f increases which further results in increased efficiency.
3. Prevention to convection losses also increases the efficiency.

Hence it can be said that efficiency of HPVT system can be increased by considerable amount by optimizing the values of different energies with the help of modification in the design of system. So for doing those modifications some designs are represented in Fig 3.9 to 3.12.

3.7 EVOLUTION OF PROPOSED MODIFIED DESIGN

Proposed design for modified model is made on paper and will be designed on CFD software for further analysis. The schematic of these proposed designs are represented here in the following diagrams.

Fig. 3.9: Basic Model With Panel And Absorbing Plate Placed Over Duct.

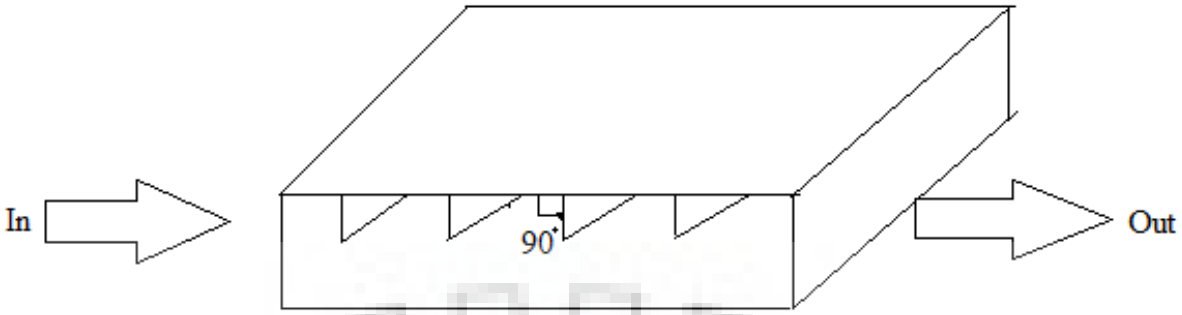

Fig. 3.10: Simple Duct (Without Panel and Absorbing Plate) With Ribs at 90°.

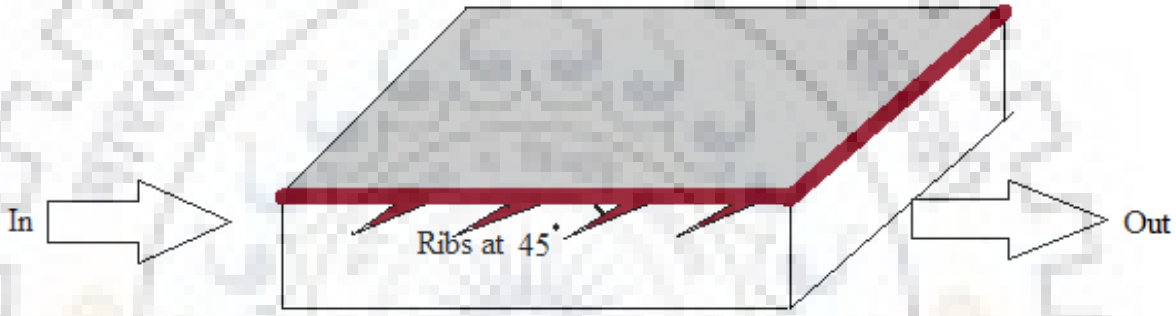

Fig. 3.11: Modified Duct Having Panel And Absorbing Plate With Ribs At 45°.

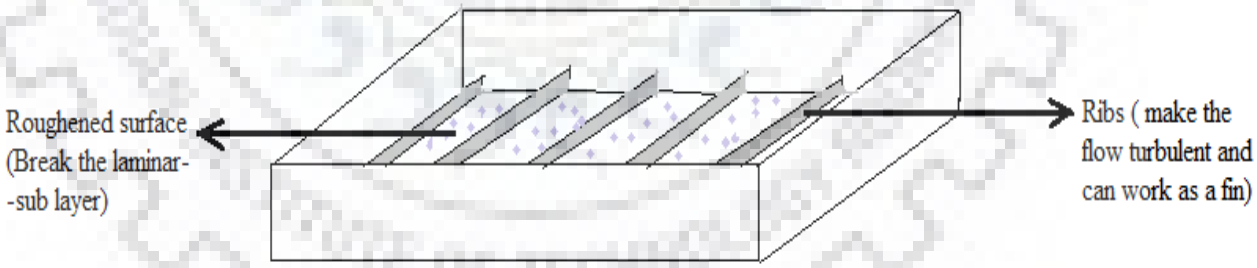

Fig. 3.12: Modified Inverted Duct With Ribs And Roughened Surface.

After making those modifications with the help of line diagrams, proper dimensions with several specifications are required for a realistic analysis of HPVT system. For that purpose, sizing of HPVT system is done here, which is as follows:

3.8 SIZING OF SYSTEM

Details for sizing of HPVT system, parameters, boundary conditions, electrical, mechanical and thermal specifications used for data reduction are discussed below.

3.8.1 Parameters Used For Analysis of HPVT System

Following parameters and materials for construction are taken for the analysis of HPVT system.

1. Length of duct = 1640mm.
2. Width of duct = 1000mm.
3. Depth of duct = 100mm.
4. Hydraulic Diameter- 182mm.
5. Thickness of absorbing plate = 1mm.
6. Material of absorbing plate = Aluminium.
7. Wall material for insulation = Wood.
8. Length of solar panel = 1640mm.
9. Width of solar panel = 981mm.

3.8.2 Boundary Conditions

1. Temperature of heated panel- 333K.
2. Wall temperature- 300K.
3. Type of heat transfer fluid- Air.
4. Velocity of HTF at inlet- 0.1-0.5 m/s.
5. Ambient temperature- 300K.
6. Reynold Number- 1200-7200.
7. Kinematic viscosity of Air- 1.49×10^{-5} Ns/m^2.
8. Incident solar radiation- 1000 W/m^2.

Electrical specification of the standard module used for the analysis of HPVT system are given below in Table 3.2.

Table 3.2: Electrical Specification Considered for A Standard Module of HPVT System.

S. No.	Electrical Specifications	Values
1.	Open circuit voltage (V)	36.8
2.	Short circuit current (A)	8.40
3.	Maximum power P_{max} (W)	230
4.	Maximum power voltage V_{mp} (V)	29.30
5.	Maximum power current I_{mp} (A)	7.85
6.	Module efficiency (%)	>14
7.	Fill factor	>0.74
8.	NOCT (˚C)	47±2
9.	Temperature coefficient for I_{sc} ,(α)	+ 0.46 mA/˚C
10.	Temperature coefficient for V_{oc} ,(β)	-2.1 mV/˚C
11.	Temperature coefficient for Power, (ϒ)	-0.44%/˚C
12.	Standard test condition (STC)	1000 W/m^2, 25˚C, AM 1.5

Mechanical specification of the standard module and duct used for the analysis of HPVT system are given below in Table 3.3.

Table 3.3: Mechanical Specification of a Standard Module and Duct.

S. No.	Mechanical Specifications	Values
1.	Module dimensions	(L×W×H) 1640×981×40 (mm)
2.	Length of duct	1640 mm
3.	Width of duct	1000 mm
4.	Depth of duct	100 mm
5.	Thickness of absorbing plate	1 mm
6.	Material of absorbing plate	Aluminum
7.	Weight	18.3 kg
8.	Material of insulation	Wood
9.	Thickness of insulation	10 mm

Thermal Properties of different component used for HPVT system are given below in Table 3.4.

Table 3.4: Thermal Properties of Module, Duct and Fluid Used.

S. No.	Part of HPVT System	Material	Thermal Property	Value
1.	Absorber Plate	Aluminium	Thermal Conductivity	205 W/m K
2.	Insulation	Wood	Thermal Conductivity	0.09 W/m K
3.	Ambient Air	Air	Convective Coefficient	10 W/m^2 K
4.	HTF	Air	Specific Heat (Cp)	1005 J/KgK
5.	Module	Si,Al,Glass	Overall Specific Heat	770 J/KgK

After analyzing the factors and parameters which affects the heat transfer rate in HPVT system, some modifications are done in basic model which are shown earlier with the help of line diagram. Now these line diagrams are designed in ANSYS with proper dimensions, parameters and boundary conditions for further analysis. The design made on ansys of those line diagram which were discussed earlier, are shown below.

3.9 MODIFIED DESIGNS ON THE BASIS OF PARAMETER FOUND

Different types of modified designs made on ANSYS 15.0 are given below:

3.9.1 Duct with Spherical Shaped Protrusion

For the first modification, spherical shaped protrusions are made on the absorbing plate which is placed below the solar panel. These spherical protrusion increase the heat transfer from absorber plate and hence reduce the temperature of solar panel, which will finally increase the overall efficiency of heated panel.

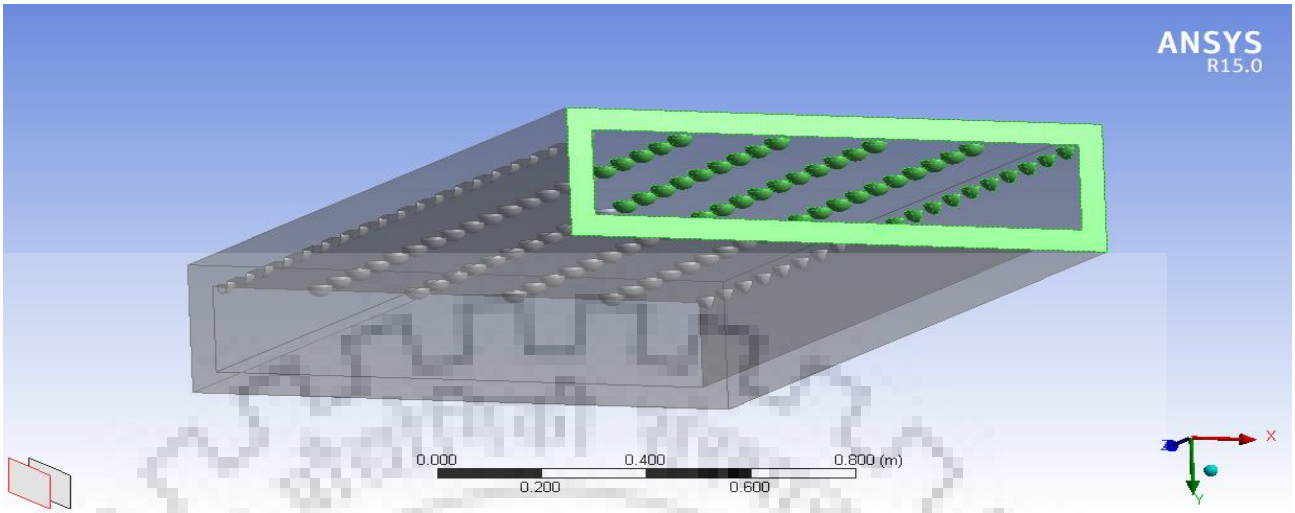

Fig. 3.12: Duct With spherical shaped protrusion.

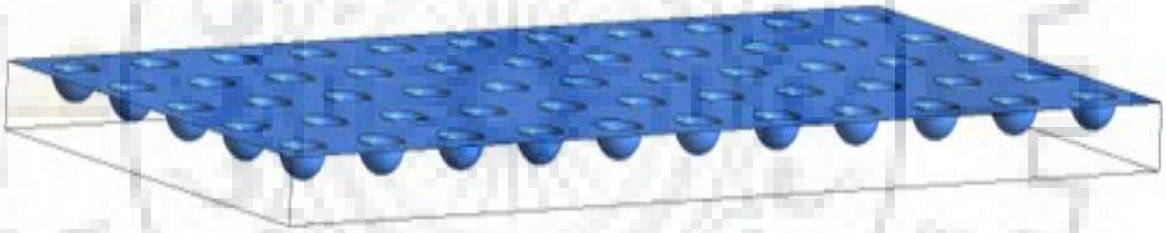

Fig. 3.13: Duct With spherical shaped protrusion.

3.9.2 Duct with Cubical Shaped Protrusion

Now those spherical shaped protrusions are replaced by cubical shaped protrusion made on the absorbing plate as shown in Fig 3.14 and 3.15 which is placed below the solar panel. These cubical protrusion increase the heat transfer from absorber plate and reduce the temperature of solar panel. Which will again increase the overall efficiency of heated panel but the amount of change in efficiency will be the factor to be noticed here.

With this change in design, effect on different efficiencies will be seen in the later part of this dissertation work with the help of CFD analysis.

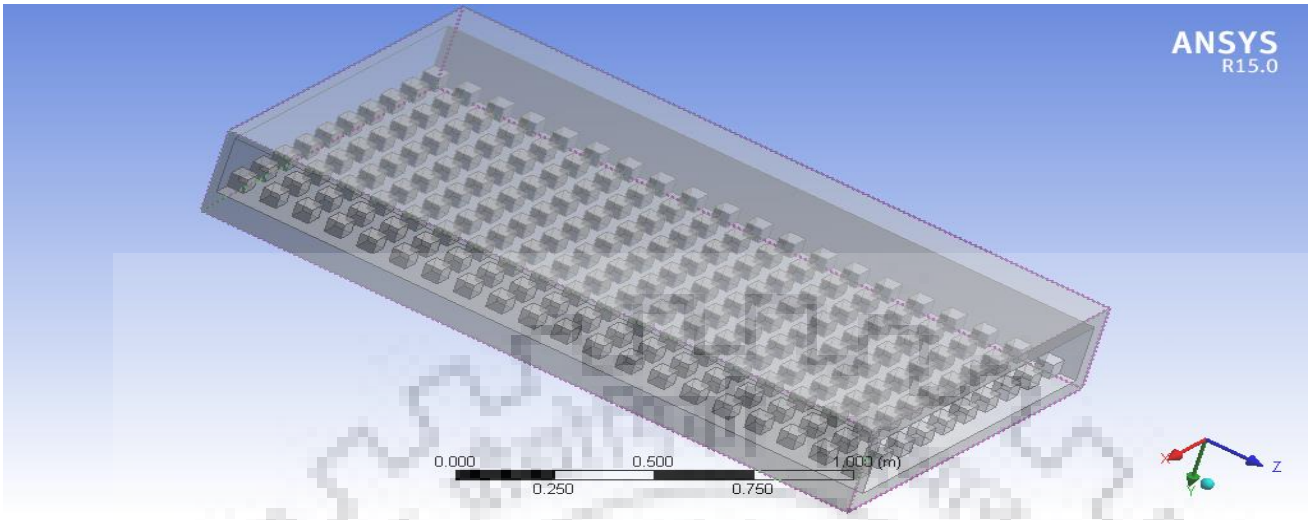

Fig. 3.14: Duct (upside down) with cubical shaped protrusion.

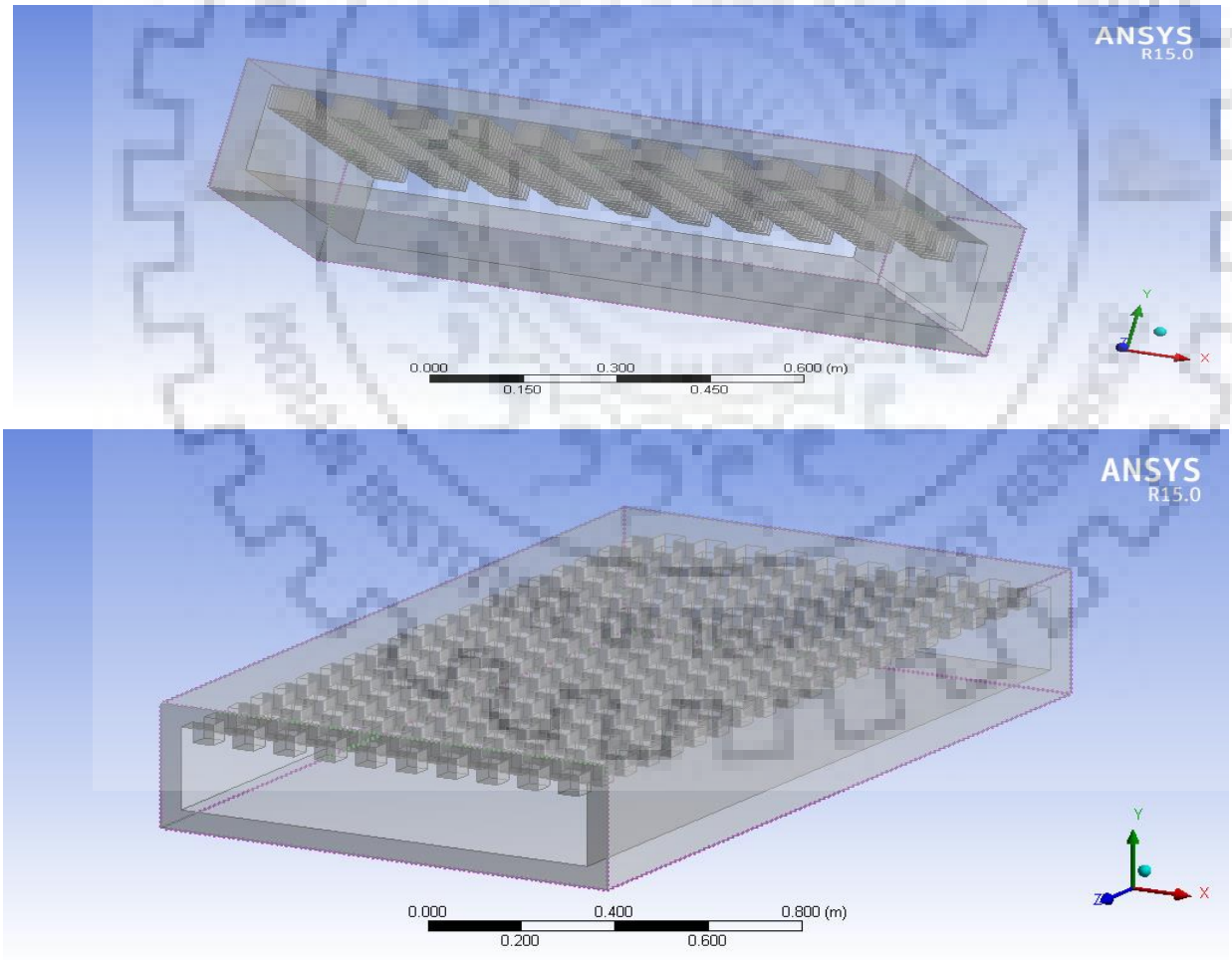

Fig. 3.15: Duct with cubical shaped protrusion.

3.9.3 Duct with Ribs Angle at 90° (Longitudinal and Transverse)

After those intermittent protrusions some continuous roughness or ribs are introduced for further modification testing, here those intermittent protrusions are replaced by the continuous ribs which are perpendicular to the absorbing plate, placed below the solar panel. These perpendicular ribs increase the heat transfer from absorber plate and hence reduce the temperature of solar panel. Which will finally increase the overall efficiency of heated panel. With this change in design, effect on overall efficiency will be seen later with the help of CFD analysis. Following Fig. 3.18 and Fig. 3.19 and Fig. 3.21 show the longitudinal and transverse types of perpendicular ribs respectively.

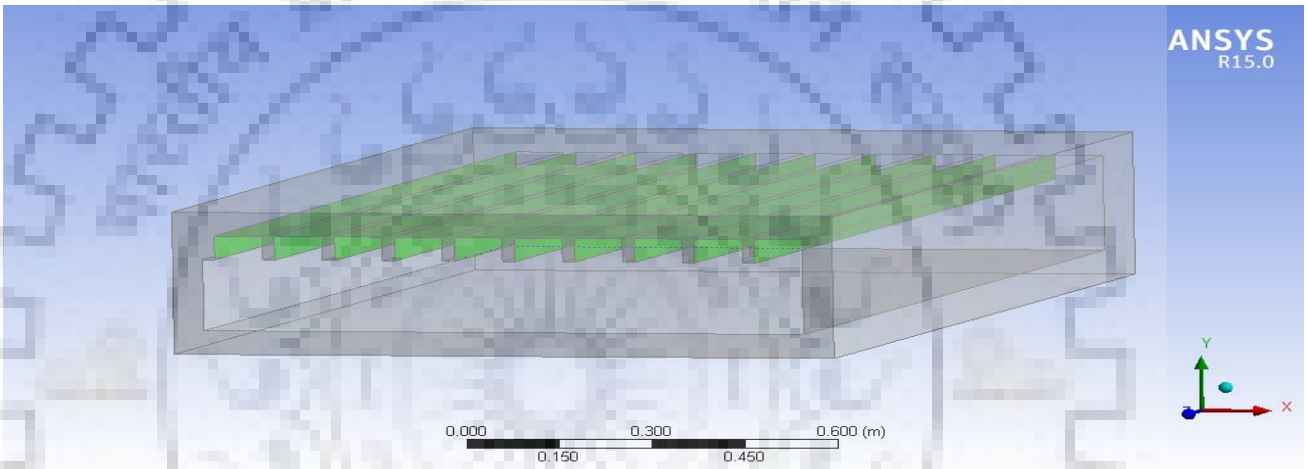

Fig. 3.16: Duct with Ribs at angle 90° (Longitudinal).

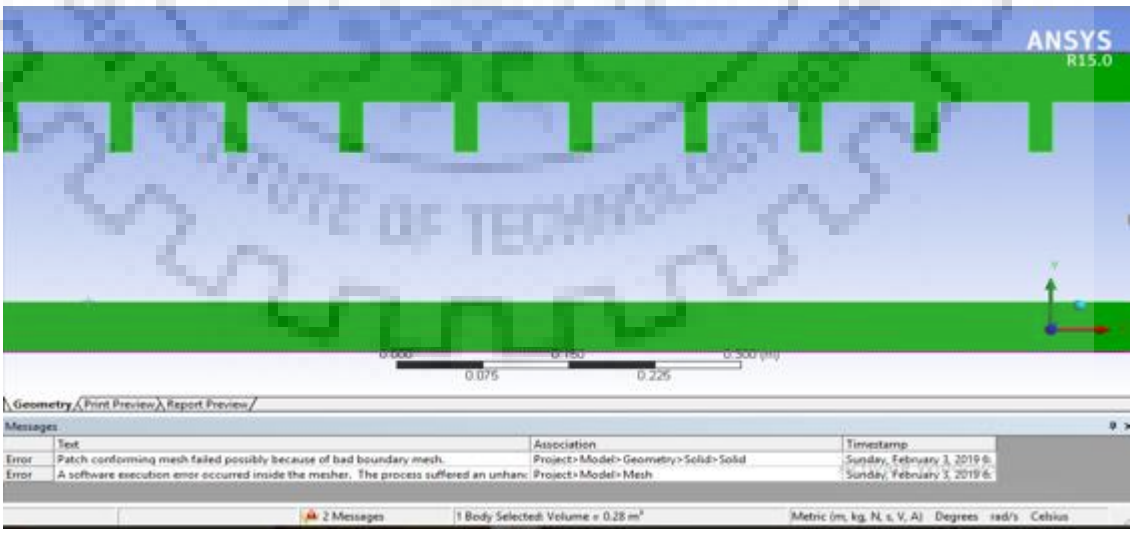

Fig. 3.17: Simple Duct With Transverse Ribs at 90°.

3.9.4 Duct with Ribs at an Angle of 45°

After those continuous perpendicular ribs some continuous roughness but at an angle of 45° are introduced for further modification testing, to the absorbing plate, placed below the solar panel. These 45° ribs increase the heat transfer from absorber plate and hence reduce the temperature of solar panel. Which will finally increase the overall efficiency of heated panel again. With this change in design, effect on overall efficiency will be seen with the help of CFD analysis. Fig. 3.20 shows the duct having ribs at an angle of 45°.

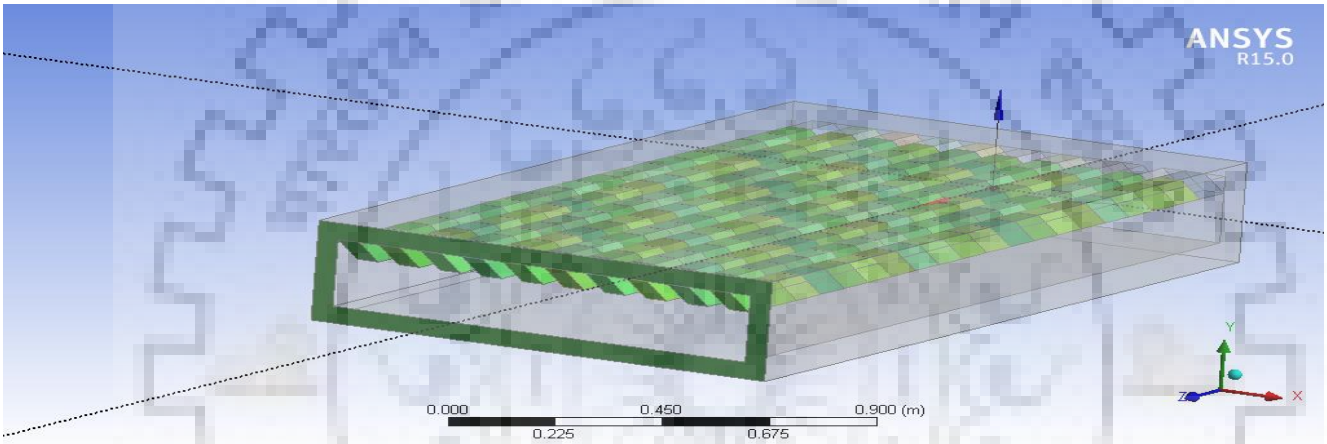

Fig. 3.18: Duct with Ribs at an angle 45°.

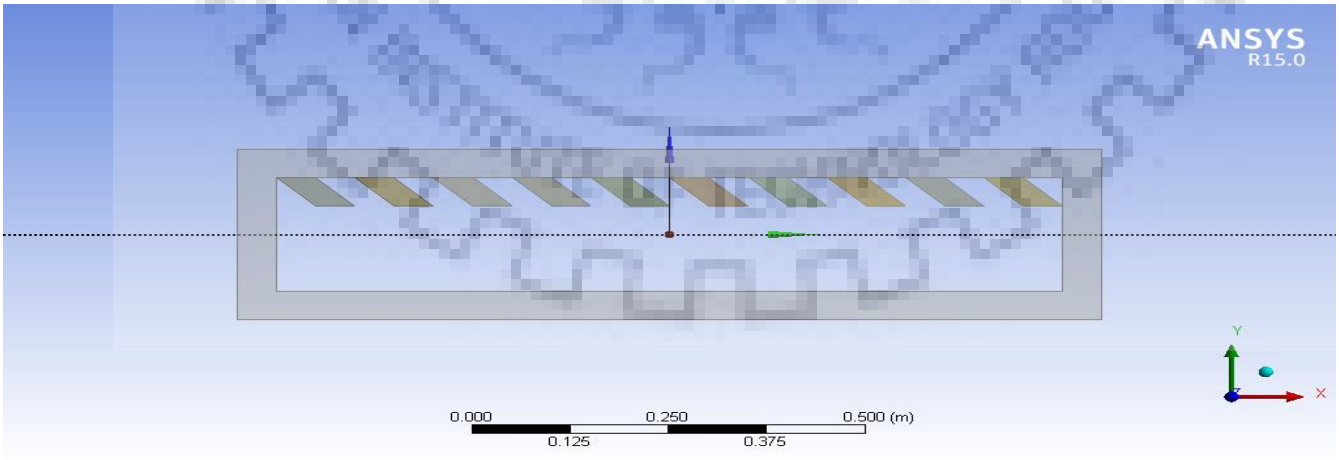

Fig. 3.19: Sectional view of Duct with Ribs at an angle 45°.

3.10 MESHING OF MODIFIED DESIGNS

After making those designs in CFD software (ansys) , next step is to break the whole system into several small elements to find the solutions. This is done by creating the mesh within the syatem, called meshing of system. In the Fig. 3.22 to 3.24 some meshed system are shown there with meshing details.

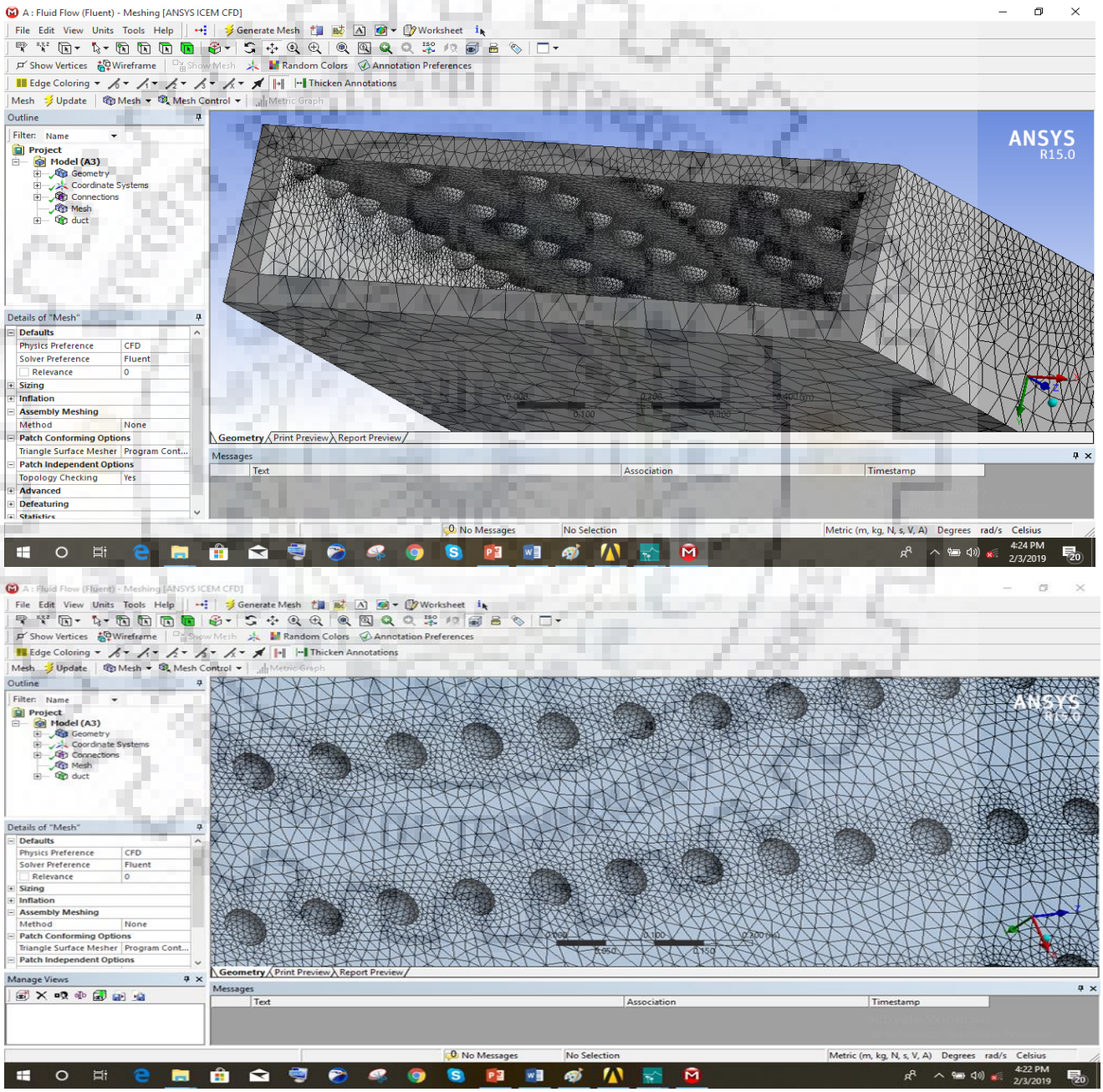

Fig. 3.20: Meshing of fluid domain with spherical shaped protrusion.

Details of "Mesh"	
Sizing	
Use Advanced Size Fun...	On: Curvature
Relevance Center	Coarse
Initial Size Seed	Active Assembly
Smoothing	Medium
Transition	Slow
Span Angle Center	Fine
Curvature Normal A...	Default (18.0 °)
Min Size	Default (1.2056e-003 m)
Max Face Size	Default (0.120560 m)
Max Size	Default (0.241110 m)
Growth Rate	Default (1.20)
Minimum Edge Length	0.10 m
Inflation	
Assembly Meshing	
Patch Conforming Options	
Triangle Surface Mesher	Program Controlled
Patch Independent Options	
Topology Checking	Yes
Advanced	
Defeaturing	
Statistics	
Nodes	121477
Elements	617436
Mesh Metric	None

Fig. 3.21: Meshing Details of fluid domain with spherical shaped protrusion.

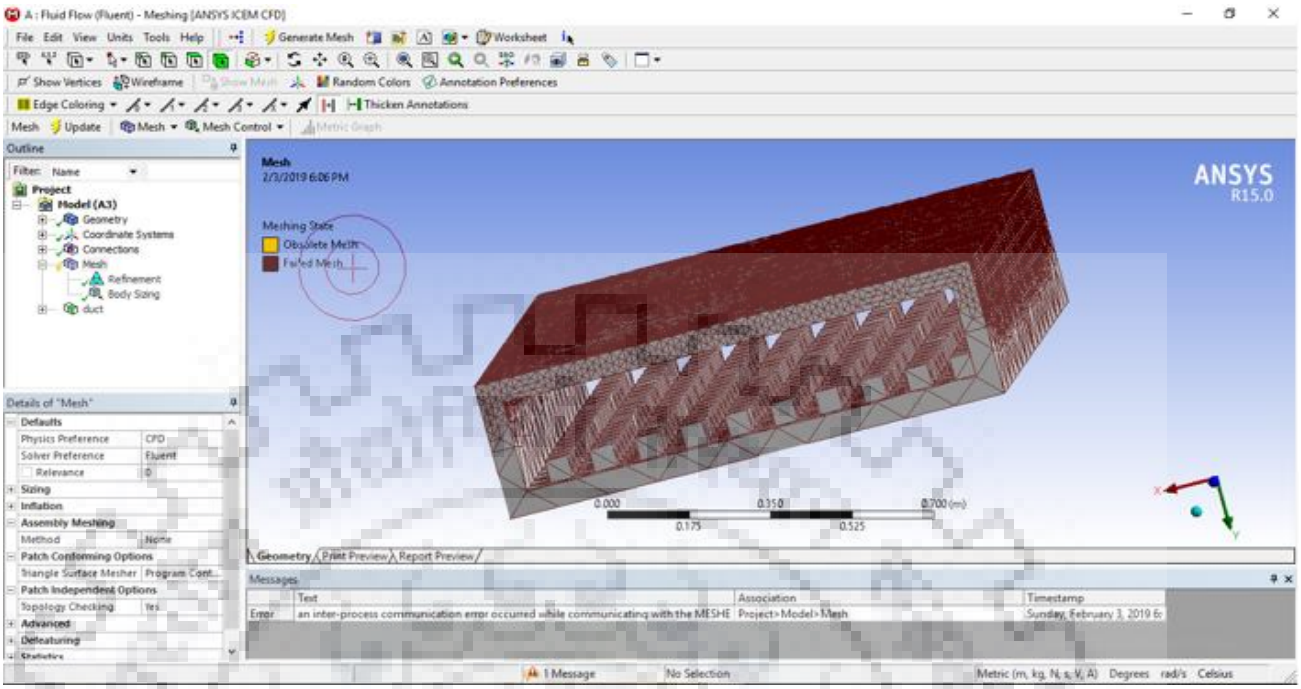

Fig. 3.22: Meshing of a duct having cubical shaped protrusion.

3.11 SOLVER SETUP AND BOUNDARY CONDITIONS FOR MODIFIED SYSTEMS

After the meshing, some boundary conditions and initial conditions are being set under the solver setup in Ansys. Some of those major setups are shown below in Table 3.5 for the fluid domain for duct having spherical shaped protrusions which is also shown in Fig 3.25.

Table 3.5: Solver Setup Parameters.

S. No.	Parameters	Type
1.	General setup of model	Pressure based (absolute)
2.	Selection of turbulence model	k-epsilon, standard model used
3.	Cell zone condition setup	Fluid (Air) is used
4.	Solution method	SIMPLEC
5.	Solution initialization	Hybrid initialization (Computed from all zones)
6.	No. of iterations	500-1000 (Depending upon the complexity)

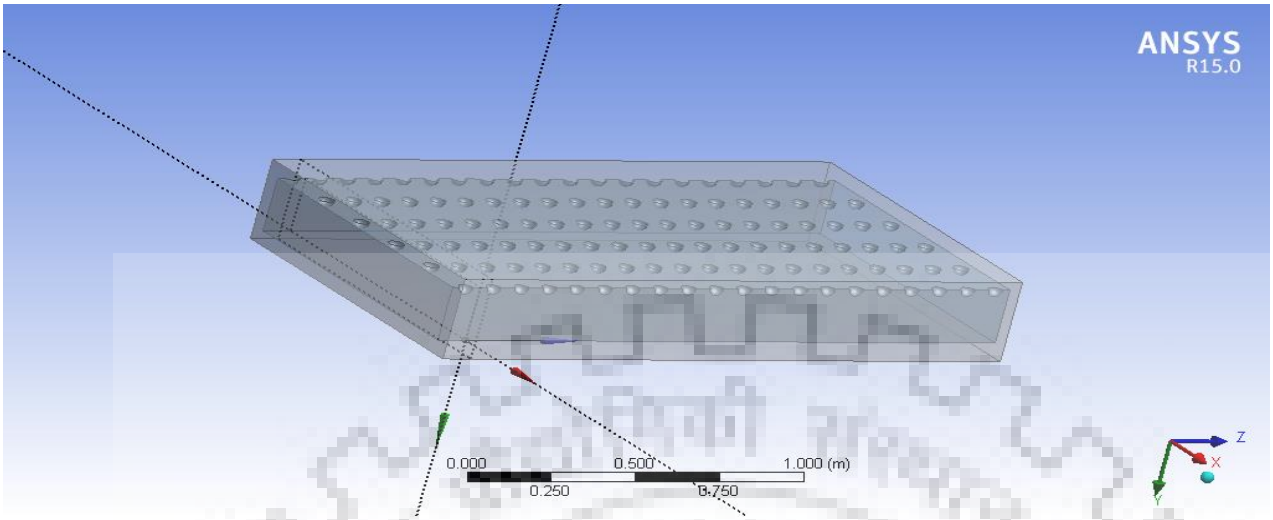

Fig. 3.23: Fluid domain of duct having spherical shaped protrusions.

Similarly, fluid domain is considered for all other modified systems for analysis on CFD. After getting those required data from CFD, some formulae are used to get specific results for comparison of basic system and modified systems, those formulae and calculations are given below in the form of data reduction and calculations.

3.12 DATA REDUCTION

1. Area of cross section of duct (A) = $W \times D$.
2. Hydraulic diameter (D_h) = $2 \times W \times D/(W+D)$.
3. Velocity of air (v) = $(Re \times \mu)/\rho \times D_h$.
4. Density of air (ρ) = 1.2 Kg/m^3.
5. Kinematic viscosity of air (μ_{air}) = 1.5 x 10^{-5} Ns/m^2.
6. Mass flow rate ($\dot{m}$) = $\rho \times A \times V$.

3.13 CALCULATIONS

For the calculation of different types of energy and efficiency several assumptions are considered to reduce the complexity and making the calculations feasible, those assumptions are given below.

3.13.1 Considered Assumptions for Analysis of Modified System

1. Neglect losses through duct (perfect insulation).
2. Radiation losses are neglected.
3. Steady state analysis.
4. Energy generation (Volumetric) is zero, i.e, E_{gen} =0
5. Reflectivity of solar panel (ρ) =0
6. Total radiation falling on solar panel is converting into 3 kinds of energies, i.e. electrical energy, thermal energy and convection losses, so the energy equation can be written in the form of equation 3.10.

$$E_{in} + E_{gen} = E_{out} + \text{losses} \quad (3.10)$$

Where,

E_{gen} = 0, therefore equation 3.10 can be written as;

$E_{in} = E_{out}$ + losses

Therefore,

Es + Ep = Ee + Ef + Convection Losses

Where,

Es = solar energy absorbed by pannel

Ep = energy required to drive the pump

Ee = electrical power generated by panel

E_f = energy carried away by fluid

Now, the system efficiency, electrical efficiency and thermal efficiency can be written in the form of energy inputs and outputs (in watts) as:

$$\eta s = \frac{energy\ output\ from\ HPVT\ system}{energy\ input\ to\ the\ HPVT\ system} = \frac{Ee + Ef}{Es + Ep}$$

$$\eta e = \frac{Electrical\ energy\ output}{Energy\ input\ to\ the\ system} = \frac{Ee}{Es}$$

$$\eta th = \frac{Thermal\ energy\ extracted}{Energy\ available\ \ to\ the\ system} = \frac{Eth}{Es - conv.losses}$$

System efficiency (ηs) can be increased by optimizing the values of energies in the given formula for efficiency. Here in the above equations it can be analyzed that, Es depends upon location and it is fixed for a particular location, value of Ep is also fixed for a given mass flow rate, Ee is also

constant for a particular panel at a given temperature, now the only energy we can change is E_f (i.e. energy carried away by fluid), this is the energy which is being capitalized during this dissertation work, and ideally the maximum possible amount of this energy (that can be extracted as a thermal energy) would be equal to the convection losses to atmosphere when the panel was at maximum temperature (i.e. when there is no HTF is used).

Convection losses from the solar panel can be given by equation 3.11.

Losses = Convective losses, $L_f = h \times A \times (Tp - Ta)$ (in Watts) (3.11)

Where,

h = Convective heat transfer coefficient = 10 W/m^{2}K (atmospheric air).

A = Exposed surface area of panel =1.64×1 = 1.64 m^2 (As per model design).

Tpm = Maximum panel temperature = 333K.

Ta = ambient temperature = 300K.

Then,

Maximum convection losses, E_L (max) = h×A× (Tpm-Ta) = 541.2 W (3.12)

3.13.2. Formulae Used for Calculating Energies and Powers

As per equation 3.6 efficiency can be written as:

$$\eta = \frac{Ee + Ef}{Es + Ep}$$

So, for calculating the different values of efficiency, it is required to calculate all powers separately which is mentioned below.

3.13.2.1. Calculation for electrical power output

Ee = electrical power generated by panel can be calculated by equation 3.12.

$Ee = P_{max} - \Upsilon$ (3.12)

Where,

P_{max} is Maximum Power Rating of Panel = 230 W

Υ is Temperature coefficient of Power = -0.44%/˚C

Typical modules, which can measure approximately 1 m × 2 m or 3 ft 3 in × 6 ft 7 in, will be rated from 75 W to 350 W, depending on their efficiency so here a module is taken which has an electrical output rating (Ee) as 230 W at an operating temperature of 50℃.

Now, if the operating temperature is reduced by some amount, electrical output will automatically increase according to its temperature coefficient. Typical silicon solar panels have a

temperature coefficient of nearly -0.4 to -0.5 % (-0.44%/˚C in case of module consider for the analysis). This means that for every degree Celsius above 25, the power output from the module would drop by that percentage. So if the panel temperature will be reduced, Ee will rise as per the temperature coefficient of the panel.

3.13.2.2. Calculation of incident solar energy

Es = solar energy absorbed by panel = (1-ρ) AI (Watt) (3.13)

As per assumption,

ρ = Overall reflectivity of panel = 0.

I = Total solar radiation (Beam+ Diffused) falling on panel = 1000 W/m^2.

Therefore,

Es = solar energy absorbed by panel= AI = 1.64*1000 = 1640 W.

3.13.2.3 Calculation of pumping power

Applying Bernauli's equation for Pump or Blower at inlet (1) and outlet (2) to calculate the head developed by pump and hence to calculate power. So Bernauli's equation can be written in the form of equation 3.15.

$(P_1 + p_{atm}) / \rho g + (V_1)^2 / 2g + Z_1 = P_{atm} / \rho g + (V_2)^2 / 2g + Z_2$ (3.15)

Solving this equation 3.15 for the values of $Z_1 = Z_2$ and $V_1 = 0$, gives equation 3.16.

$P_1 / \rho g = (V_2)^2 / 2g = H$ (3.16)

By equation 3.16 it can be said that, (P_1 / rg) is the pressure head (energy) required at inlet to give an outlet velocity of V_2 , which is further the inlet velocity for the duct of HPVT system. So with the help of equation 3.16, the pumping power (Ep) required to drive the pump/blower (in Watts) to give an outlet velocity of V_2 can be writeen by equation 3.17.

$Ep = \dot{m}*g*H = \dot{m}*g*(V_2)^2 / 2g = Ep = \dot{m}(V_2)^2 / 2$ (3.17)

Assuming the efficiency of blower as 50 % , then the actual power required for blower can be written as in equation 3.18.

$Ep = \dot{m}(V_2)^2 / 2*0.5 = \dot{m}(V_2)^2$ (3.18)

Since the values for pumping power comes very less as compare to incomming solar power, so for calulating the different efficiencies, we can neglect the power required for blower to pump or circulate the HTF.

3.13.2.4 Calculation of thermal energy gained by HTF

E_f = energy carried away by fluid = $h*A*(T_p-T_f) = m*c*(T_o - T_i)$ (3.14)

Where,

T_i = Inlet fluid temperature

T_o = Outlet fluid temperature

Here T_f of fluid is varying continuously from inlet to outlet of insulated duct, attached to heated panel, so it cannot be calculated directly, that's why the data for outlet temperature (T_o) and panel temperature (T_p) is collected with the help of CFD analysis of different designs under different mass flow rates.

3.13.3 Calculation of Mass Flow Rate

As the air passes through the duct, air flow rate is varied corresponding to the Reynolds number ranging from 1200 to 7200 and velocities are calculated for the given numbers, then mass flow rate can be simply calculated by given equation 3.19 as:

$\dot{m} = \rho*A*V$ (3.19)

Mass flow rate at different Reynolds number is obtained by above equation 3.19, which is given below in the Table 3.6.

Table 3.6: Velocity and Mass Flow Rate Calculations.

S. No.	Reynolds N0.	Velocity (m/s)	Density of air (kg/m3)	Cross sec. area (m^2)	Mass flow rate (kg/s)
1.	1200	0.1	1.16	0.1	0.012
2.	2400	0.2	1.16	0.1	0.024
3.	3600	0.3	1.16	0.1	0.035
4.	4800	0.4	1.16	0.1	0.047
5.	6000	0.5	1.16	0.1	0.058
6.	7200	0.6	1.16	0.1	0.069

CHAPTER 4

PERFORMANCE ANALYSIS, RESULTS AND DISCUSSIONS

4.1 GENERAL

Design and analysis of the basic model is done in earlier chapters and some parameters are found which increase heat transfer rate in these kind of systems. On the basis of these parameter which increase heat transfer rate for HPVT System, different types of modified systems are proposed for analysis. Here in this chapter the analysis of those modified system is being carried out in CFD software ANSYS 15.0 to collect the required data for further analysis and comparison among different models.

After complete performance analysis of HPVT system (both simple and modified system) on a CFD (ansys) software, all the energy interactions and three types of efficiencies (photovoltaic, thermal and system efficiencies) will be calculated for all the models (basic and modified designs). On the basis of calculated values, comparison of results for simple and modified system is carried out by analyzing the effect of the parameters which are inserted in modified systems. On the basis of analysis on these systems, results are found and finally conclusions are drawn on the basis of those results in next chapter.

4.2 OUTPUT FOR DIFFERENT TYPES OF SYSTEMS

For analysis of HPVT system values for temperatures (Panel temperature (T_p), Air inlet temperature (T_{in}), Air outlet temperature (T_{out})) at different locations are required which has been collected with the help of CFD analysis as shown below in following figures:

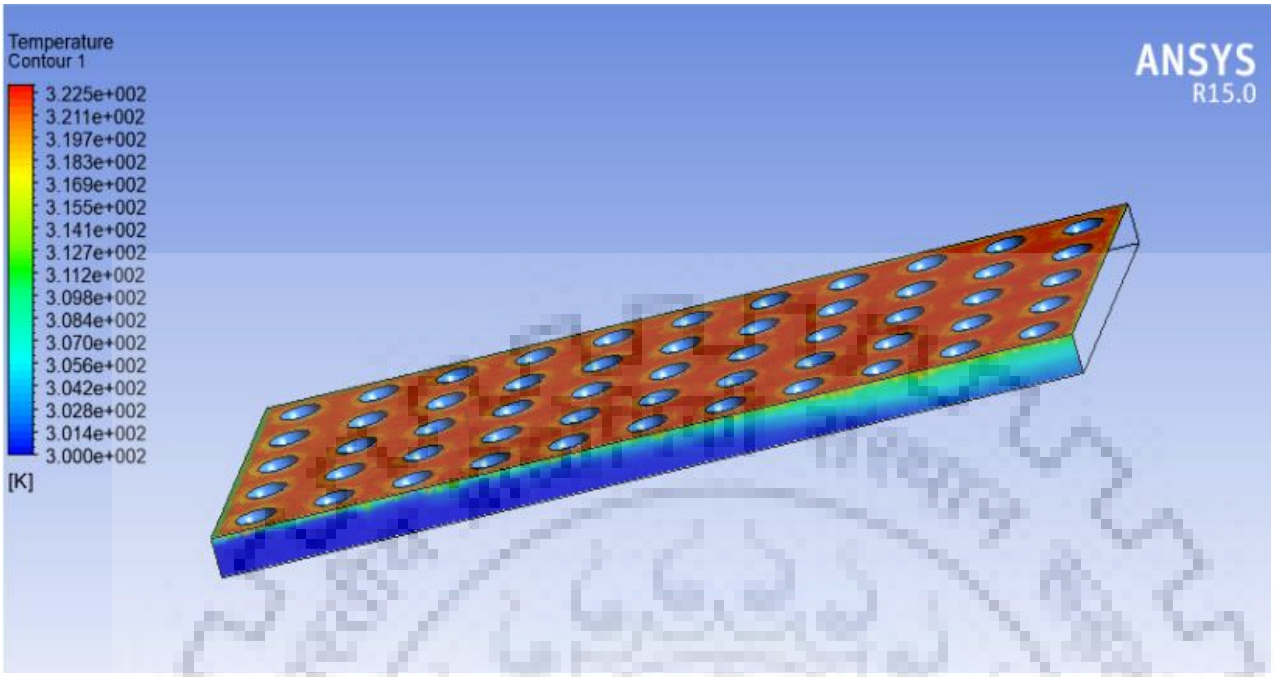

Fig. 4.1: Fluid Domain Representing Variation of Temperature along the Duct.

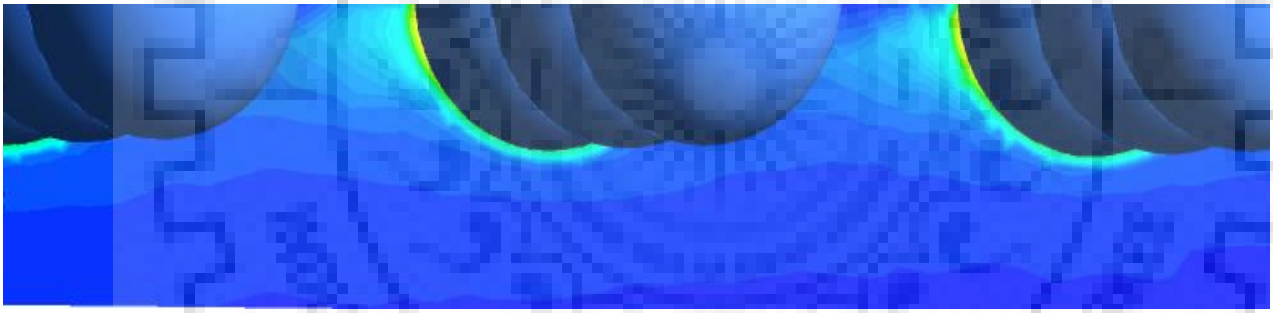

Fig. 4.2: Variation of Temperature in the Vicinity of Spherical Protrusions.

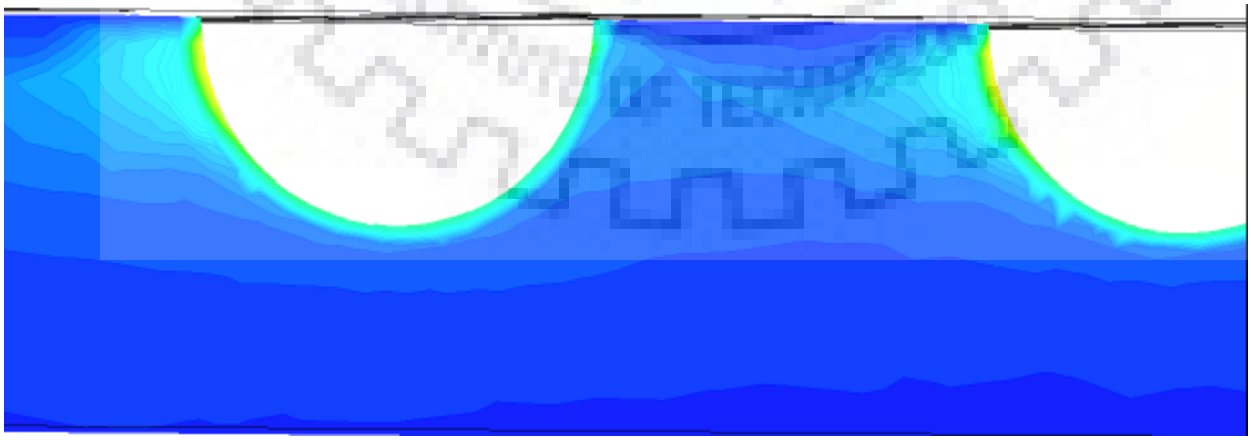

Fig. 4.3: Cross sectional view of duct with Spherical Protrusions.

Similarly, after getting all the values by conducting CFD for all other modified designs of HPVT system, values of temperatures are being noted down. Calculation for different energies and efficiency is carried out with the help of those temperatures which are represented in Table 4.1 to Table 4.12.

4.2.1 Simple Duct

Temperatures at different locations, powers and efficiency for a simple duct, is given in Table 4.1 and 4.2, graphical representation of different variations is shown in Fig 4.4 and Fig 4.5.

Table 4.1: Temperature Calculations for Simple Duct.

S. No.	Velocity (m/s)	$\dot{m}$ (kg/s)	T_p (˚C)	T_{in} (˚C)	T_{out} (˚C)	dT_f (˚C)	E_f (W)	$(dt)_p$ (˚C)	(T_p-T_a) (˚C)
1.	0	0	60	-	-	-	-	0	33
2.	0.1	0.012	59.1	27	30.11	3.11	37.5066	0.9	32.1
3.	0.2	0.024	58.5	27	29.92	2.92	70.4304	1.5	31.5
4.	0.3	0.035	57.8	27	29.15	2.15	75.6263	2.2	30.8
5.	0.4	0.047	56.9	27	28.9	1.9	89.7465	3.1	29.9
6.	0.5	0.058	55.7	27	28.47	1.47	85.6863	4.3	28.7
7.	0.6	0.069	54.7	27	28.1	1.1	76.2795	5.3	27.7

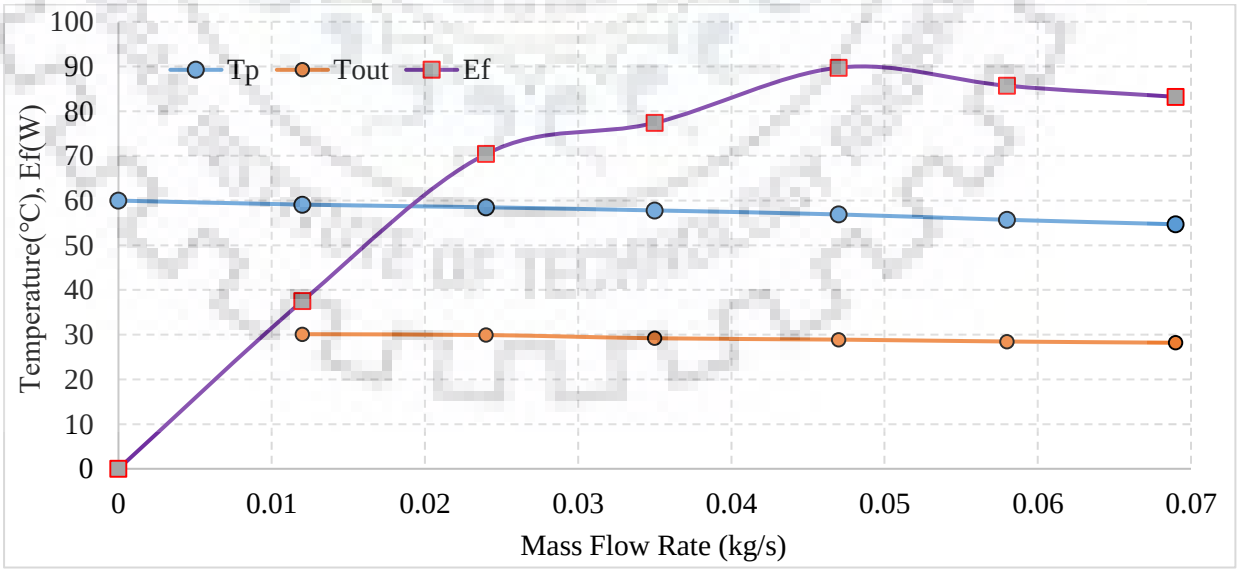

Fig. 4.4: Variation of T_p, T_o and E_f with $\dot{m}$ for simple duct.

Table 4.2: Power and Efficiency Calculations for Simple Duct.

S. No.	Velocity (m/s)	ṁ (kg/s)	Es (W)	Ee (W)	Ef (W)	Ep (W)	ηe (%)	ηt (%)	ηs (%)
1	0	0	1640	194.6	0	0	11.87	0	11.87
2	0.1	0.012	1640	195.491	37.32	0.00012	11.93	3.36	15.29
3	0.2	0.024	1640	196.098	70.08	0.00096	11.96	6.24	18.2
4	0.3	0.035	1640	196.806	75.25	0.00315	12.01	6.64	18.65
5	0.4	0.047	1640	197.717	89.3	0.00752	12.06	7.77	19.83
6	0.5	0.058	1640	198.932	85.26	0.0145	12.13	7.3	19.43
7	0.6	0.069	1640	199.944	75.9	0.02484	12.2	6.41	18.61

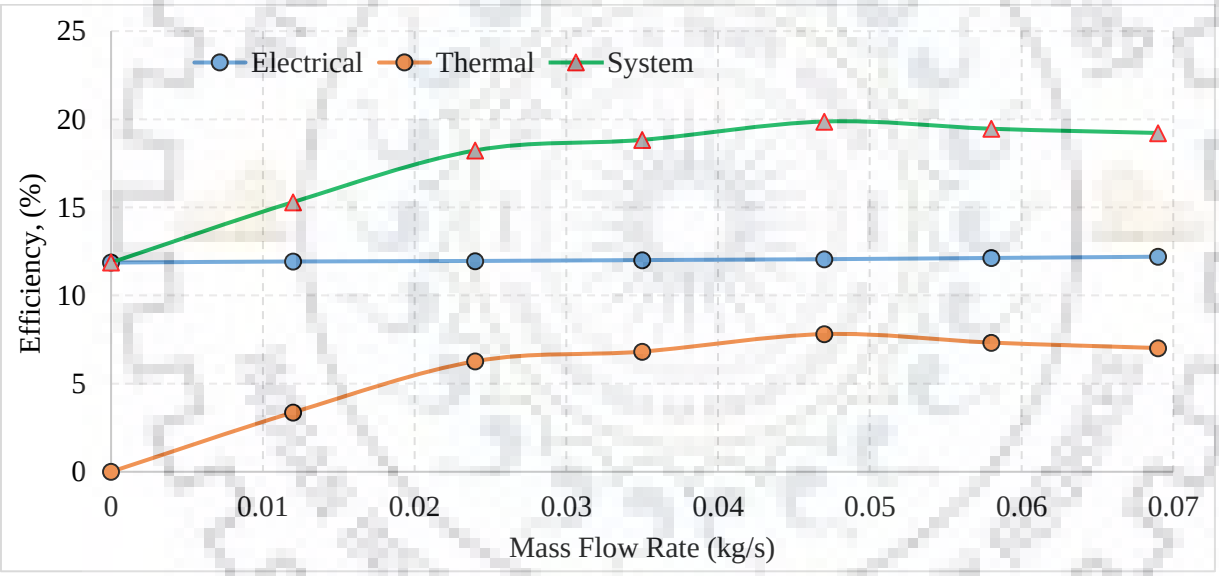

Fig. 4.5: Variation of Efficiencies with ṁ for Simple Duct.

4.2.2 Duct With Spherical Shaped Protrusions

Temperatures at different locations, powers and efficiency for the duct having Spherical Shaped Protrusions, are given in Table 4.3 and 4.4. The graphical representation of different variations is shown in Fig 4.6 and Fig 4.7.

Table 4.3: Temperature calculations for Duct with Spherical Protrusions.

S. No.	Velocity (m/s)	ṁ (kg/s)	Tp (˚C)	Tin (˚C)	Tout (˚C)	dTf (˚C)	Ef (W)	(dt)p (˚C)	(Tp-Ta) (˚C)
1.	0	0	60	-	-	-	0	0	33
2.	0.1	0.012	58.6	27	31	4	48.24	1.4	31.6
3.	0.2	0.024	57.3	27	30.03	3.03	73.0836	2.7	30.3
4.	0.3	0.035	55.6	27	30	3	105.525	4.4	28.6
5.	0.4	0.047	54	27	29.85	2.85	134.62	6	27
6.	0.5	0.058	52.7	27	29.5	2.5	145.725	7.3	25.7
7.	0.6	0.069	51.45	27	29.22	2.22	153.946	8.55	24.45

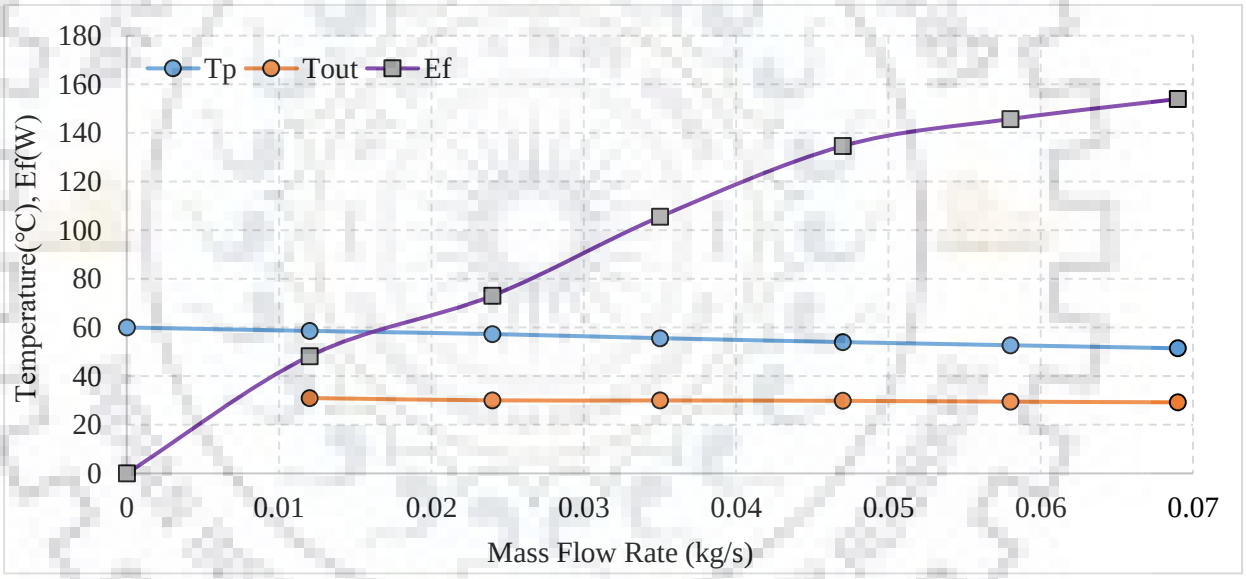

Fig. 4.6: Variation of T_p, T_o and E_f with ṁ for Spherical Protrusions.

Table 4.4: Power and Efficiency Calculations for Duct with Spherical Protrusions.

S. No.	Velocity (m/s)	ṁ (kg/s)	Es (W)	Ee (W)	Ef (W)	Ep (W)	ηe (%)	ηt (%)	ηs (%)
1.	0	0	1640	194.6	0	0	11.87	0	11.87
2.	0.1	0.012	1640	195.997	48	0.00012	11.96	4.28	16.24
3.	0.2	0.024	1640	197.312	72.72	0.00096	12.04	6.37	18.41
4.	0.3	0.035	1640	199.033	105	0.00315	12.14	8.97	21.11
5.	0.4	0.047	1640	200.652	133.95	0.00752	12.24	11.19	23.43
6.	0.5	0.058	1640	201.968	145	0.0145	12.32	11.9	24.22
7.	0.6	0.069	1640	203.233	153.18	0.02484	12.4	12.37	24.77

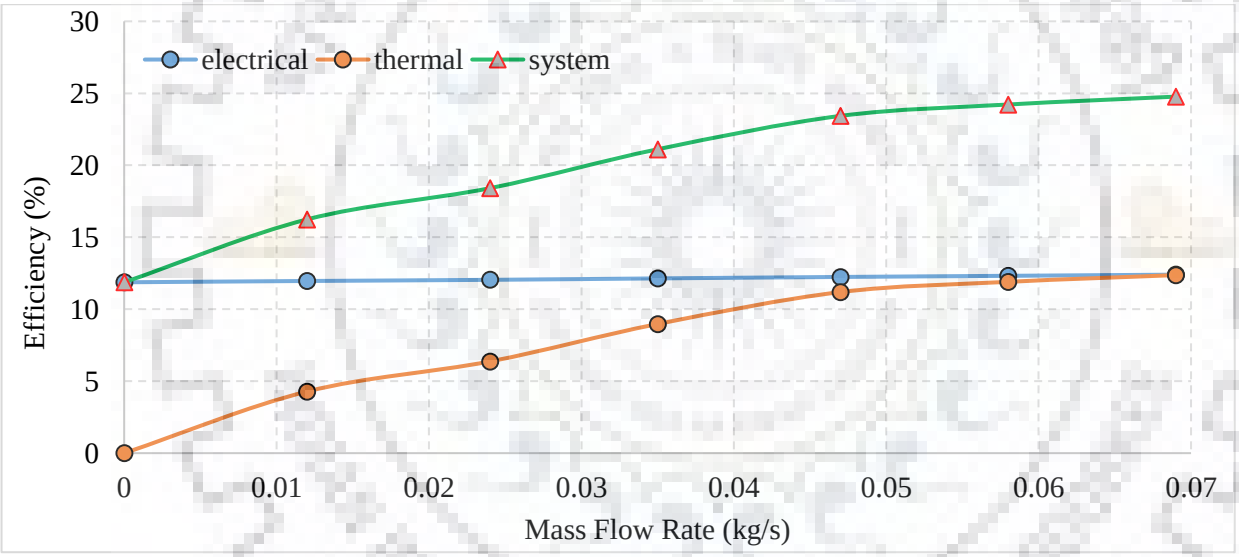

Fig. 4.7: Variation of Efficiencies with ṁ for Duct with Spherical Protrusions.

4.2.3 Duct Having Cubical Shaped Protrusions

Temperatures at different locations, powers and efficiency for the duct having Cubical Protrusions, is given in Table 4.5 and 4.6, further graphical representation of different variations is shown in Fig. 4.8 and Fig. 4.9.

Table 4.5: Temperature Calculations for Duct with Cubical Protrusions.

S. No.	Velocity (m/s)	ṁ (kg/s)	Tp (˚C)	Tin (˚C)	Tout (˚C)	dTf (˚C)	Ef (W)	(dt)p (˚C)	(Tp-Ta) (˚C)
1.	0	0	60	-	-	-	-	0	33
2.	0.1	0.012	58.8	27	30.8	3.8	45.828	1.2	31.8
3.	0.2	0.024	57	27	30.3	3.3	79.596	3	30
4.	0.3	0.035	55.1	27	30	3	105.525	4.9	28.1
5.	0.4	0.047	53.6	27	29.9	2.9	136.982	6.4	26.6
6.	0.5	0.058	51.9	27	29.7	2.7	157.383	8.1	24.9
7.	0.6	0.069	50.8	27	29.4	2.4	166.428	9.2	23.8

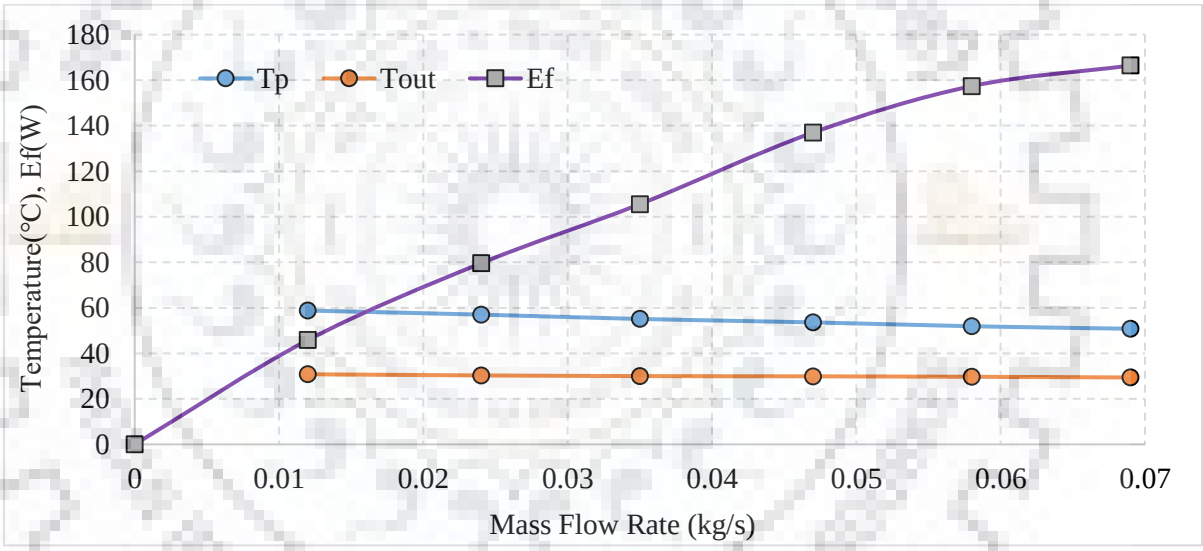

Fig. 4.8: Variation of T_p, T_o and E_f with ṁ for Duct having Cubical Protrusions.

Table 4.6: Power and Efficiency Calculations for Duct with Cubical Protrusions.

S. No.	Velocity (m/s)	ṁ (kg/s)	Es (W)	Ee (W)	Ef (W)	Ep (W)	ηe (%)	ηt (%)	ηs (%)
1.	0	0	1640	194.6	0	0	11.87	0	11.87
2.	0.1	0.012	1640	195.794	45.6	0.00012	11.94	4.08	16.02
3.	0.2	0.024	1640	197.616	79.2	0.00096	12.05	6.9	18.95
4.	0.3	0.035	1640	199.539	105	0.00315	12.17	8.91	21.08
5.	0.4	0.047	1640	201.057	136.3	0.00752	12.26	11.33	23.59
6.	0.5	0.058	1640	202.777	156.6	0.0145	12.37	12.72	25.09
7.	0.6	0.069	1640	203.89	165.6	0.02484	12.44	13.26	25.7

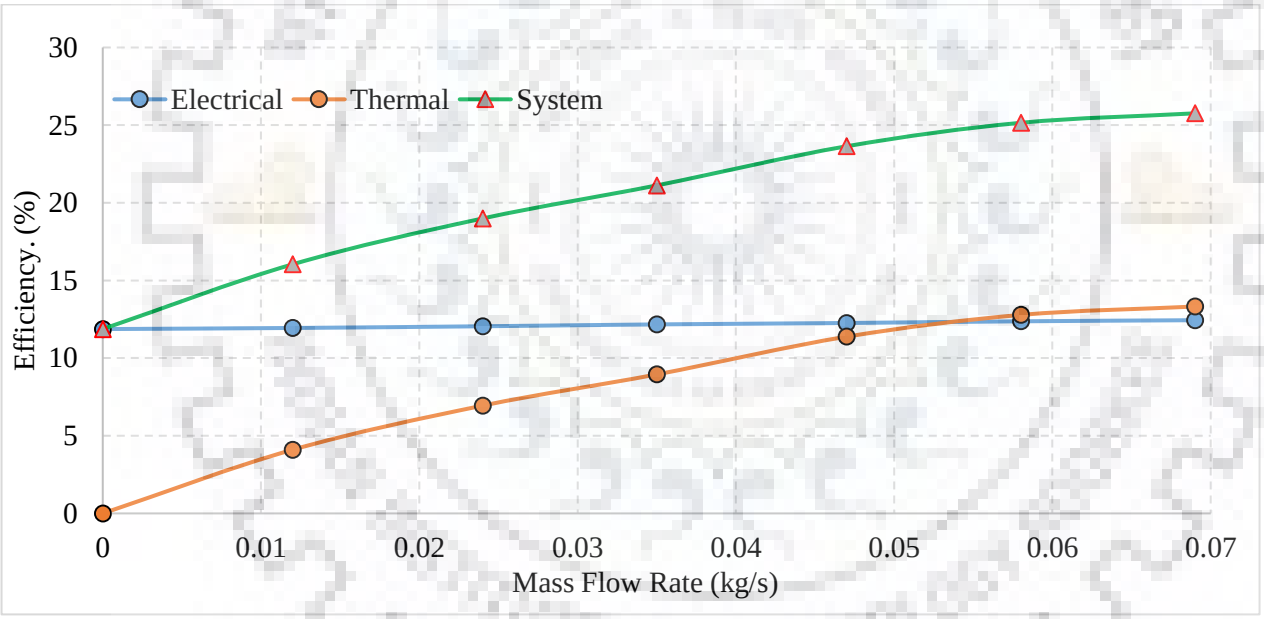

Fig. 4.9: Variation of Efficiencies with ṁ for Duct with Cubical Protrusions.

4.2.4 Duct with Longitudinal Ribs

Temperatures variation at different locations, powers and efficiency for the duct with longitudinal ribs, is given in Table 4.7 and 4.8. Graphical representation of different variations is shown in Fig. 4.10 and Fig. 4.11.

Table 4.7: Temperature Calculations for Duct with Longitudinal Ribs.

S. No.	Velocity (m/s)	ṁ (kg/s)	Tp (˚C)	Tin (˚C)	Tout (˚C)	dTf (˚C)	Ef (W)	(dt)p (˚C)	(Tp-Ta) (˚C)
1.	0	0	60	-	-	-	-	0	33
2.	0.1	0.012	59.1	27	30.52	3.52	42.4512	0.9	32.1
3.	0.2	0.024	58.3	27	29.72	2.72	65.6064	1.7	31.3
4.	0.3	0.035	57.5	27	29.45	2.45	86.1788	2.5	30.5
5.	0.4	0.047	56.5	27	29.3	2.3	108.641	3.5	29.5
6.	0.5	0.058	55.3	27	28.86	1.86	108.419	4.7	28.3
7.	0.6	0.069	54.9	27	28.5	1.5	104.018	5.1	27.9

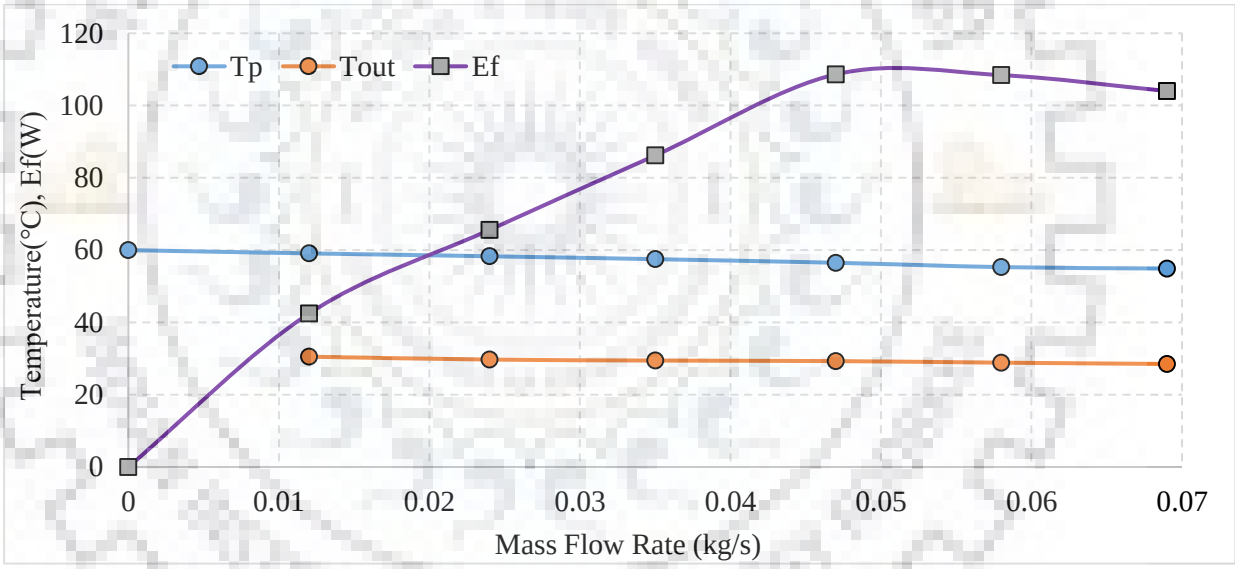

Fig. 4.10: Variation of T_p, T_o and E_f with ṁ for Duct with Longitudinal Ribs.

Table 4.8: Power and Efficiency Calculations for Duct with Longitudinal Ribs.

S. No.	Velocity (m/s)	ṁ (kg/s)	Es (W)	Ee (W)	Ef (W)	Ep (W)	ηe (%)	ηt (%)	ηs (%)
1.	0	0	1640	194.6	0	0	11.87	0	11.87
2.	0.1	0.012	1640	195.491	42.24	0.00012	11.93	3.8	15.73
3.	0.2	0.024	1640	196.3	65.28	0.00096	11.97	5.8	17.77
4.	0.3	0.035	1640	197.11	85.75	0.00315	12.02	7.53	19.55
5.	0.4	0.047	1640	198.122	108.1	0.00752	12.09	9.35	21.44
6.	0.5	0.058	1640	199.336	107.88	0.0145	12.16	9.18	21.34
7.	0.6	0.069	1640	199.741	103.5	0.02484	12.18	8.76	20.94

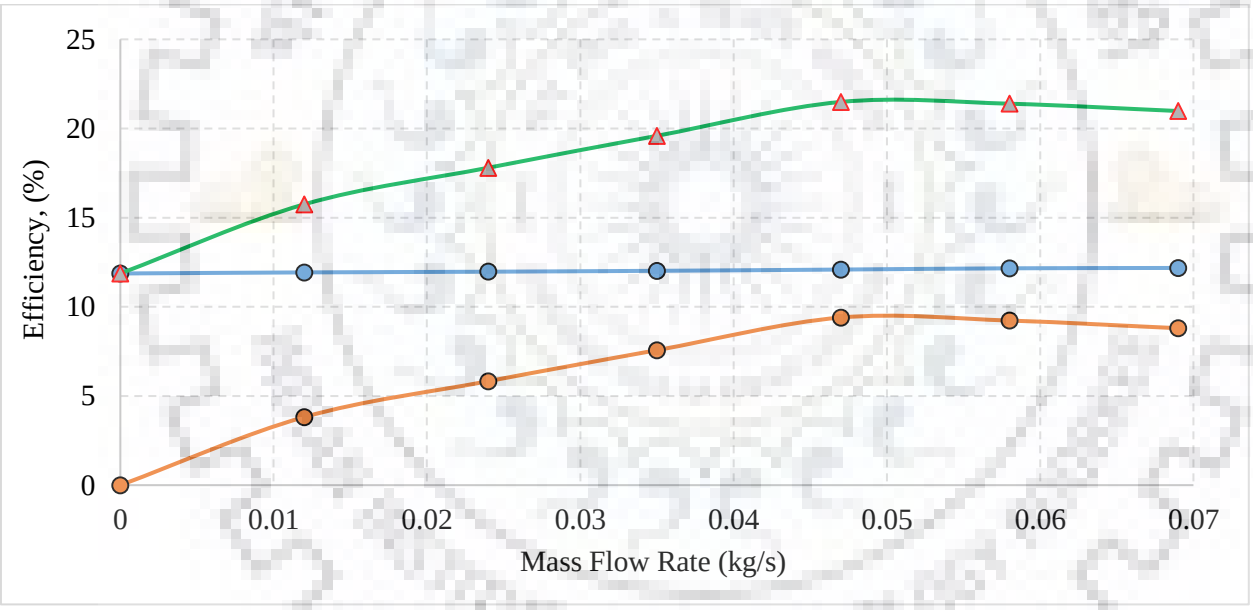

Fig. 4.11: Variation of Efficiencies with ṁ for Duct with Longitudinal Ribs.

4.2.5 Duct with Transverse Continuous Ribs

Temperatures variation at different locations, powers and efficiency for the duct with transverse ribs, is given in in Table 4.9 and 4.10, further graphical representation of different variations of energy and efficiency is shown in Fig. 4.12 and Fig. 4.13.

Table 4.9: Temperature Calculations for Duct with Longitudinal Ribs.

S. No.	Velocity (m/s)	ṁ (kg/s)	Tp (˚C)	Tin (˚C)	Tout (˚C)	dTf (˚C)	Ef (W)	(dt)p (˚C)	(Tp-Ta) (˚C)
1.	0	0.000	60	-	-	-	-	0	33
2.	0.1	0.012	59	27	29.95	2.95	35.577	1	32
3.	0.2	0.024	57.9	27	29.8	2.8	67.536	2.1	30.9
4.	0.3	0.035	56.5	27	29.55	2.55	89.6963	3.5	29.5
5.	0.4	0.047	55.4	27	29.3	2.3	108.641	4.6	28.4
6.	0.5	0.058	54.2	27	28.99	1.99	115.997	5.8	27.2
7.	0.6	0.069	53.2	27	28.62	1.62	112.339	6.8	26.2

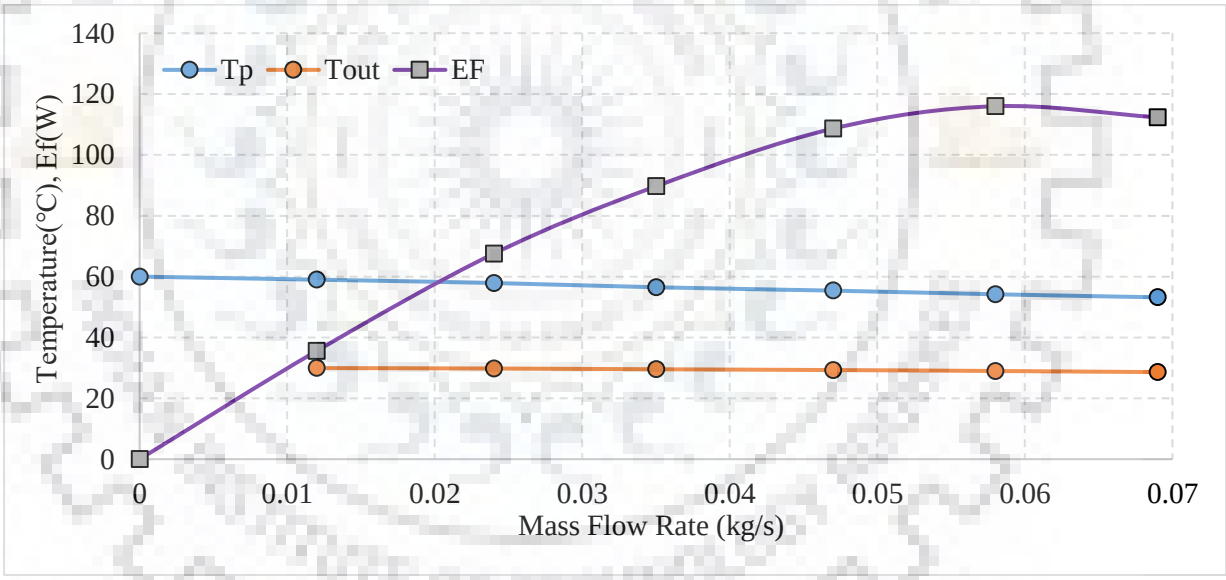

Fig. 4.12: Variation of T_p, T_o and E_f with ṁ for Duct with Transverse Ribs.

Table 4.10: Power and Efficiency Calculations for Duct with Transverse Ribs.

S. No.	Velocity (m/s)	ṁ (kg/s)	Es (W)	Ee (W)	Ef (W)	Ep (W)	ηe (%)	ηt (%)	ηs (%)
1.	0	0.000	1640	194.6	0	0	11.87	0	11.87
2.	0.1	0.012	1640	195.592	35.577	0.00012	11.93	3.2	15.13
3.	0.2	0.024	1640	196.705	67.536	0.00096	12	5.96	17.96
4.	0.3	0.035	1640	198.122	89.6963	0.00315	12.09	7.76	19.85
5.	0.4	0.047	1640	199.235	108.641	0.00752	12.15	9.26	21.41
6.	0.5	0.058	1640	200.45	115.997	0.0145	12.23	9.72	21.95
7.	0.6	0.069	1640	201.462	112.339	0.02484	12.29	9.29	21.58

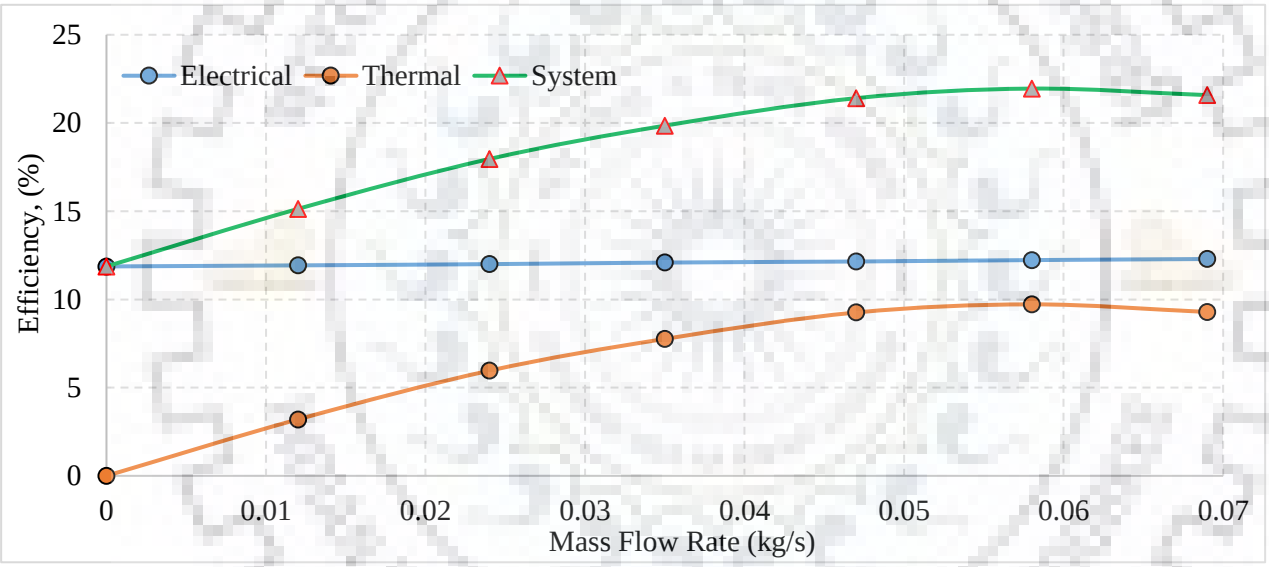

Fig. 4.13: Variation of Efficiencies with ṁ for Duct with Transverse Ribs.

4.2.6 Duct with Ribs at an angle 45°

Temperatures at different locations, powers and efficiency for the duct having Ribs at an angle 45°, is given in Table 4.11 and 4.12. The graphical representation of different variations is shown in Fig. 4.14 and Fig. 4.15.

Table 4.11: Temperature Calculations for Duct with Ribs at an Angle 45°.

S. No.	Velocity (m/s)	ṁ (kg/s)	Tp (˚C)	Tin (˚C)	Tout (˚C)	dTf (˚C)	Ef (W)	(dt)p (˚C)	(Tp-Ta) (˚C)
1.	0	0.000	60	-	-	-	-		33
2.	0.1	0.012	58.8	27	30.2	3.2	38.592	1.2	31.8
3.	0.2	0.024	57.5	27	30.02	3.02	72.8424	2.5	30.5
4.	0.3	0.035	56.1	27	29.81	2.81	98.8418	3.9	29.1
5.	0.4	0.047	54.4	27	29.6	2.6	122.811	5.6	27.4
6.	0.5	0.058	53.3	27	29.25	2.25	131.153	6.7	26.3
7.	0.6	0.069	52.6	27	29	2	138.69	7.4	25.6

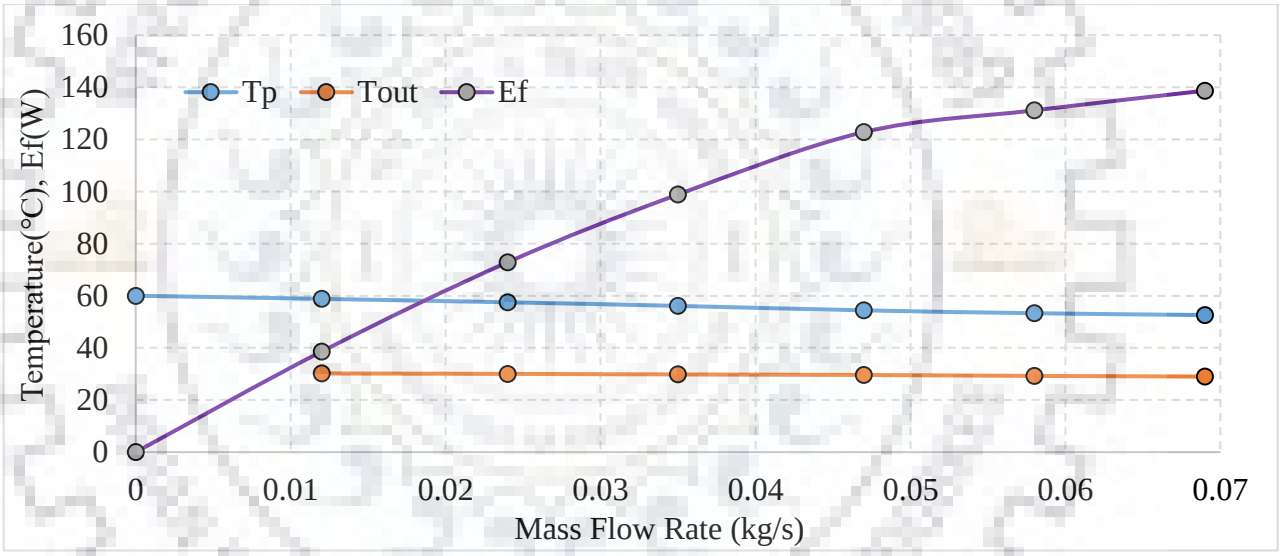

Fig. 4.14: Variation of Tp, To and Ef with ṁ for Duct with Ribs at an angle 45°.

Table 4.12: Power and Efficiency Calculations for Duct with Ribs at an Angle 45°.

S. No.	Velocity (m/s)	ṁ (kg/s)	Es (W)	Ee (W)	Ef (W)	Ep (W)	ηe (%)	ηt (%)	ηs (%)
1.	0	0.000	1640	194.6	0	0	11.87	0	11.87
2.	0.1	0.012	1640	195.794	38.592	0.00012	11.94	3.46	15.4
3.	0.2	0.024	1640	197.11	72.8424	0.00096	12.02	6.4	18.42
4.	0.3	0.035	1640	198.527	98.8418	0.00315	12.11	8.51	20.62
5.	0.4	0.047	1640	200.247	122.811	0.00752	12.22	10.32	22.54
6.	0.5	0.058	1640	201.36	131.153	0.0145	12.28	10.86	23.14
7.	0.6	0.069	1640	202.069	138.69	0.02484	12.33	11.37	23.7

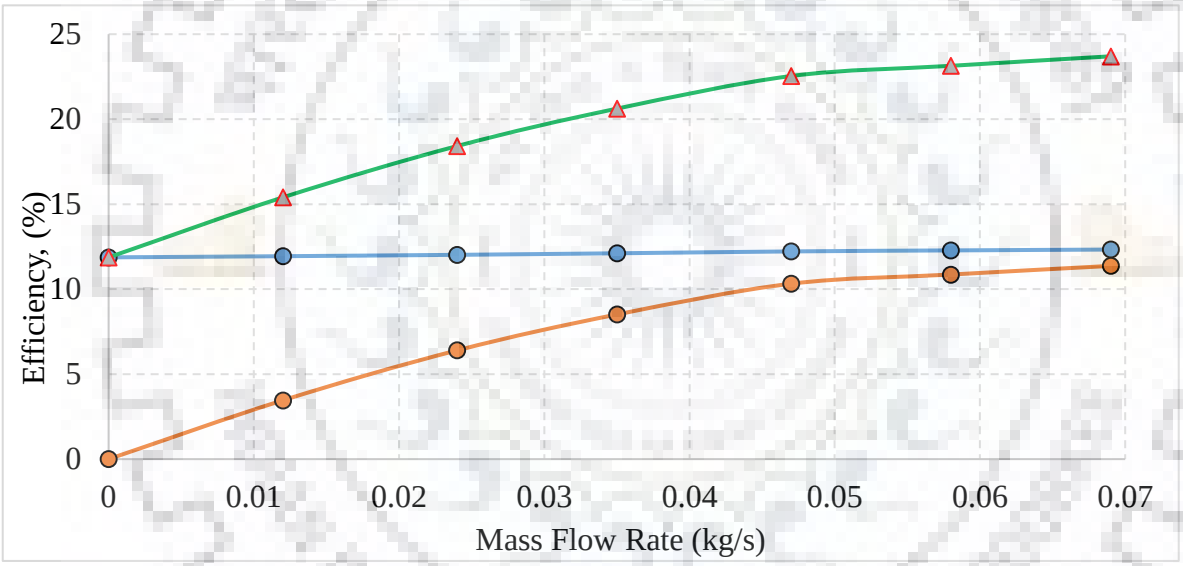

Fig. 4.15: Variation of Efficiencies with ṁ for duct with Ribs at an angle 45°.

4.3 DISCUSSION OVER THE VARIATION OF TEMPERATURE, POWERS AND EFFICIENCIES

With the help of previous analysis, it can be seen that mass flow rate is varied from 0.012 kg/s to 0.069 kg/s. As the mass flow rate is increased, the panel temperature is reduced for all the different modified designs of HPVT system. It can also be seen that, by increasing the mass flow rate, both thermal and electrical power output is increased, but the thermal power output is increasing rapidly as compared to electrical power.

There is also an increase in all three kind of efficiencies (Thermal, Electrical and system efficiency) with an increased mass flow rate up to 0.069 kg/s. Highest reduction in panel temperature is found 9.2 ℃ and the highest increment in electrical efficiency was about 4.8 %, both in the case of HPVT system having duct with cubical shaped protrusions, with a maximum mass flow rate of 0.069 kg/s.

It is also found that the rate of decrease in convection losses is almost same as the rate of increment in the thermal energy carried away by fluid (Ef), which shows their inverse proportion relationship. After the analysis same type of pattern for variation is found in all types of HPVT system, the variation for the HPVT system having duct with cubical protrusions is shown in Fig. 4.16.

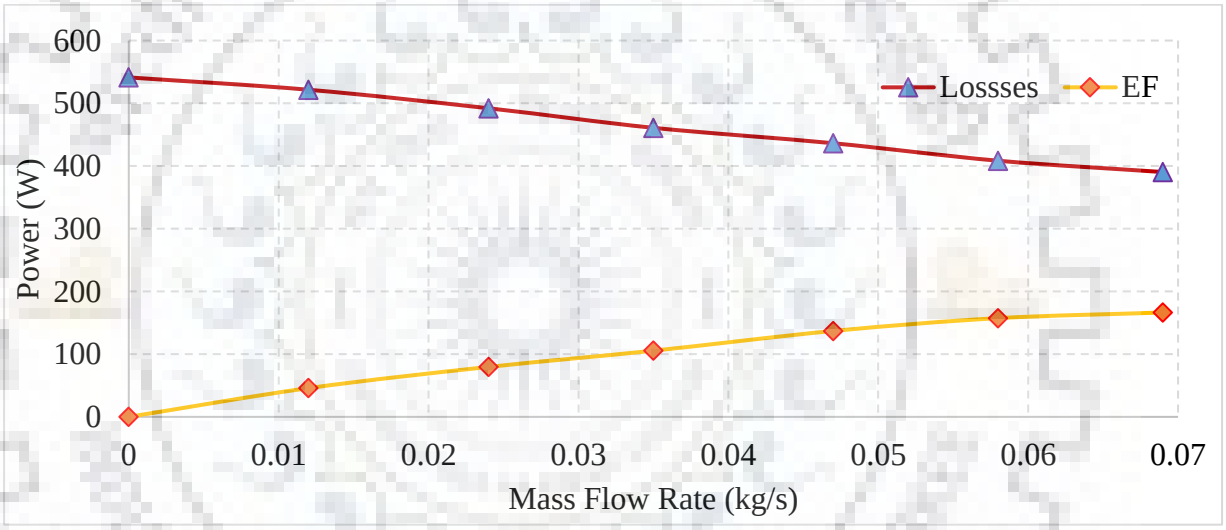

Fig. 4.16: Variation of Convection Losses and E_f with Mass Flow Rate.

After increasing the mass flow rate beyond 0.069 (i.e. Reynold number beyond 7200), there is not a significant increment in powers and efficiency, but this value may change according to system and HTF used. The comparison of different system is given in Table 4.13 and shown in Fig. 4.17.

Table 4.13: Comparison of Panel temperature and PV Efficiency for Different Systems.

S. No.	Heat transfer Fluid (HFT) used.	ṁ (kg/s)	Tp (°C)	(dT)p (°C)	% Increase in PV (Electrical) efficiency
1.	Without HFT	0.000	60.0	0	0
2.	Simple duct	0.069	54.7	5.3	2.7 %
3.	Duct With spherical protrusions	0.069	51.45	8.55	4.5 %
4.	Duct With cubical shaped protrusion	0.069	50.8	9.2	4.8 %
5.	Duct With longitudinal ribs	0.069	54.9	6.1	2.9 %
6.	Duct With transverse continuous ribs	0.069	53.2	6.8	3.5 %
7.	Duct with Ribs at an angle 45°	0.069	52.6	7.4	3.9 %

Table 4.14: Comparison of Efficiencies for different systems.

S. No.	Type of HPVT system.	ṁ (kg/s)	Electrical efficiency %	Thermal efficiency %	System efficiency %
1.	Without HFT	0.000	11.87	0.00	11.87
2.	Simple duct	0.069	12.20	6.41	18.61
3.	Duct With spherical protrusions	0.069	12.40	12.37	24.77
4.	Duct With cubical shaped protrusion	0.069	12.44	13.26	25.70
5.	Duct With longitudinal ribs	0.069	12.18	8.76	20.94
6.	Duct With transverse continuous ribs	0.069	12.29	9.29	21.58
7.	Duct with Ribs at an angle 45°	0.069	12.33	11.37	23.70

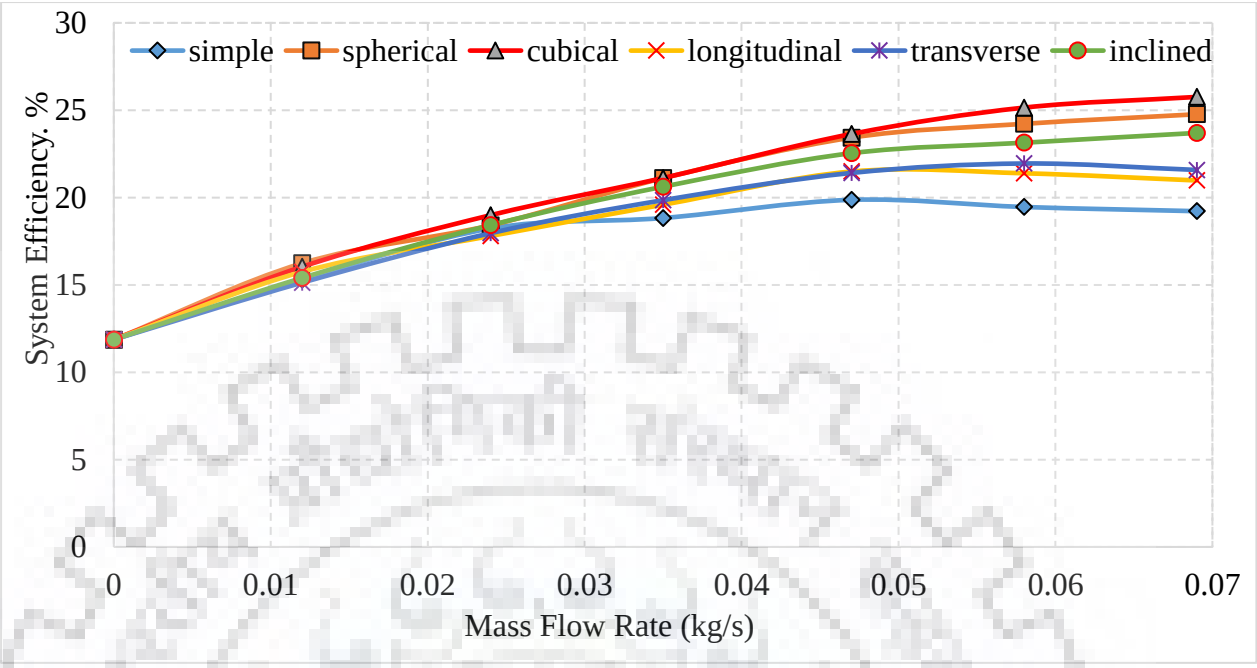

Fig. 4.17: Comparison of System Efficiencies of Different Designs.

As HPVT systems with discontinuous roughness of cubical and spherical shape having a system efficiency of 25.70% and 24.77%, and systems having continuous ribs in longitudinal, transverse and inclined direction have an efficiency of 20.94 %, 21.58 % and 23.7% respectively at a mass flow rate of 0.069 kg/s. So, it can be summarized as, at higher mass flow rate, system having discontinuous ribs or protrusions are more efficient than those having continuous ribs, and the reduction in panel temperature is also more in case of discontinuous ribs.

CHAPTER 5
CONCLUSIONS

5.1 CONCLUSIONS

Under the present dissertation work, major factors and parameters which can affect the performance of HPVT system have been found. On the basis of those parameters, different types of HPVT systems have been designed to improve the performance of the system. CFD analysis is conducted to get the effect of variation of parameters. The following conclusions are drawn on the basis of analysis done under this dissertation work:

1. For basic model design, it is found that there is change of 1.1°C in temperature of incoming and outgoing fluids with the maximum mass flow rate of 0.069 kg/s, which implies that fluid is carrying quite less heat from the heated panel, therefore there is a need for the modification in the design of working model, which can increase the heat carrying capacity of flowing fluid (HTF) and hence performance of HPVT system.
2. For all considered systems, if the mass flow rate in increased from zero to 0.069 kg/s, rate of decrement in panel temperature is more as compare to rate of decrease in outlet temperature of HTF.
3. The maximum reduction in panel temperature of 9.2 °C and maximum increment in electrical (PV) efficiency of 4.8% is found in case of cubical shaped protrusions, whereas a 2.9 % enhancement in electrical efficiency was found with longitudinal ribs arrangements, so cubical protrusions are more efficient than the longitudinal arrangement of ribs.
4. With the increase of mass flow rates of HTF, the rate of decrease in convection loss is found to be equals to the increment in thermal power. So it can be concluded that, thermal power gained by fluid is inversely proportion to the convection loss.
5. At maximum mass flow rate of 0.069 kg/s, HPVT system having continuous ribs with longitudinal, transverse and inclined direction shows the system efficiency of 20.94 %, 21.58 % and 23.7% respectively, whereas the systems with discontinuous roughness with cubical and spherical shaped protrusions have a system efficiency of 25.70% and 24.77% respectively, therefore it is concluded that HPVT systems having discontinuous roughness are more efficient than system having continuous ribs.

5.2 RECOMMENDATIONS

There is a lot of work which can further be done in future, some of those are recommended here as:

1. More work is required to be done to find out the optimum value of hydraulic diameter, roughness height and mass flow rate for further improvement in these systems.
2. Different types of heat transfer fluid can be tested for better performance of HPVT systems.

REFERENCES

[1] http://mechanicalinventions.blogspot.com/2014/05/ [Accessed on 01.07.2018].

[2] http://www.ren21.net/gsr-2018/ [Accessed on 20.8.2018].

[3] H. Khurana;"Experimental investigation of hybrid solar photovoltaic thermal collector"; Dissertation submitted for the award of Master of Technology in AHES, AHEC IIT Roorkee (2016).

[4] Mohd. Insha; "experimental study on performance of a double pass solar air heater"; Dissertation submitted for the award of Master of Technology in AHES, AHEC IIT Roorkee (2016).

[5] R.P. Saini and J. Verma "Heat transfer and friction factor correlations for a duct having dimple-shape artificial roughness for solar air heaters" AHEC, IIT Roorkee,2007

[6] Catalin George et al. "Efficiency improvements of pv panels by using air cooled sinks" (2015).

[7] H. Khurana;"Experimental investigation of hybrid solar photovoltaic thermal collector"; Dissertation submitted for the award of Master of Technology in AHES, AHEC IIT Roorkee (2016).

[8] Mohd. Insha; "experimental study on performance of a double pass solar air heater"; Dissertation submitted for the award of Master of Technology in AHES, AHEC IIT Roorkee (2016).

[9] S. Tiwari; "experimental investigation of packed bed solar thermal storage having large size packing materials"; Dissertation submitted for the award of Master of Technology in AHES, AHEC IIT Roorkee (2016).

[10] A.K. Bhargava, H.P. Garg and R.K. Agarwal; "Study of a hybrid solar system-solar air heater combined with solar cells" (1991).

[11] T. Bergene and O.M. Lovvik; "Model calculations on a flat-plate solar heat collector with integrated solar cells", (1995).

[12] K. Sopian; K.S Yigit, H.T. Liu, S. Kaka and T.N. Veziroglu; "Performance analysis of Photovoltaic Thermal air heaters", (1996).

[13] J.K. Tonui and Y. Tripanagnostopoulos; "Performance improvement of PVT solar collectors with natural airflow operation", (2008).

[14] A. Ibrahim, M.Y. Othman, M.H. Ruslan, S. Mat and K. Sopian; "Recent advances in flat plate photovoltaic/thermal (PVT) solar collectors", (2011).

[15] N. Aste, C.D. Pero and F. Leonforte; "Water flat plate PV–thermal collectors: A review", (2014).

[16] S. Sharma, R.Singh and B. Bhushan; "CFD based investigation on effect of roughness Element pitch on performance of artificial roughness duct used in solar air heater", (2011).

[17] A. Makki, S. Omer and H. Sabir; "Advancements in hybrid photovoltaic systems for enhanced solar cells performance", (2015).

[18] T. Takashima, T. Anaka, J. Kamoshida; T. Tani and T. Horigome; "New proposal for Photovoltaic-Thermal solar energy utilization method", (1994).

[19] T.T. Chow Bilbao, I. Jose; "A review on photovoltaic/thermal hybrid solar technology", (2009).

[20] P.G. Charalambous, G.G. Maidment, S.A. Kalogirou and K. Yiakoumetti, "Photovoltaic thermal (PVT) collectors: A review", (2007).

[21] R. Santbergen, C.C.M. Rindt and R.J. Zolingen; "improvement of the performance of pvt collectors"; 5th European Thermal-Sciences Conference, The Netherlands (2008).

[22] E.M.A Alfegi, K. Sopian, M.Y. Othman and B.B. Yatim; "transient mathematical model of both side single pass photovoltaic thermal air collector", (2007)

[23] B. Hayakashi, K. Mizusaki, T.Satoh and T.Hatanaka; "Research and development of photovoltaic/thermal hybrid solar power generation system", (1990).

[24] M.Y. Othman, B. Yatim, K. Sopian and M.N. Bakar; "double-pass photovoltaic thermal solar collector", (2006).

[25] M.A. Amraoui, and K. Aliane; "Numerical analysis of a three dimensional fluid flow in a flat plate Solar collector", (2014).

[26] A.K. Kapardar and R. P. Sharma; "Numerical and CFD based analysis of porous media solar air heater", (2012).

[27] V. Katekar, B. Ankur, C. B. Kale; "Enhancement of Convective Heat Transfer Coefficient in solar Air Heater of Roughened Absorber Plate", (2010).

[28] https://www.solar-payback.com/technology/ [Accessed on 03.09.2018].

[29] https://energyintransition.wordpress.com/2013/06 [Accessed on 01.10.2018].

[30] M. Bambrook, S. Mae; "Investigation of photovoltaic / thermal air systems to create a zero energy house in Sydney" (2009).

[31] A. Garg; “development of improved receiver cavity of a solar thermal power plant”; Dissertation submitted for the award of Master of Technology in AHES, AHEC IIT Roorkee (2016).

[32] T. Norbu;”Development of hybrid energy system in Rubesa, Bhutan”; Dissertation submitted for the award of Master of Technology in AHES, AHEC IIT Roorkee (2016).

[33] A. Gupta;”Modelling of hybrid energy system”; Dissertation submitted for the award of Master of Technology in AHES, AHEC IIT Roorkee (2016).

[34] P. Saxena and D.K.khatod;”Optimized operation of hybrid power generation system” (2016).

[35] K. Kumar; “energy and exergy analysis for heliostat based solar thermal power plant”; Dissertation submitted for the award of Master of Technology in AHES, AHEC IIT Roorkee (2016).

[36] G. Cheng and Lixi Zhang; “Numerical simulation of solar air heater with V-groove absorber used in HD desalination”, (2010).